Detailed fault and fracture characterization with the latest seismic attributes techniques.

By

Isaac Ignacio González González

Student ID: 4522818

in partial fulfilment of the requirements for the degree of

Master of Science
In Petroleum Engineering and Applied Earth Sciences
at the Delft University of Technology,
to be defended publicly on May 23, 2018 at 13:00 PM.

Supervisor	Prof. Giovanni Bertotti	TU Delft
Thesis committee	Prof. Giovanni Bertotti	TU Delft
	Prof. Allard W. Martinius	TU Delft
	Dr.ir. Guy Drijkoningen	TU Delft

Title: Detailed fault and fracture characterization with the latest seismic attribute techniques.

Author	Isaac Ignacio Gonzalez Gonzalez *I.I.GonzalezGonzalez@student.tudelft.nl* Faculty of Civil Engineering and Earth Sciences Delft University of Technology
Date	May 23, 2018
Thesis supervisor	Prof. Giovanni Bertotti Head of Section Department of Geosciences and Engineering Delft University of Technology
Co-advisor	M.Sc. Farrukh Qayyum dGB Earth Sciences
Committee Members	Prof. Allard W. Martinius Geology section TU Delft Dr.ir. Guy Drijkoningen Applied Geophysics Section TU Delft

An electronic version of this thesis is available at http://repository.tudelft.nl/.

Reservoir Geology, Department of Applied Geology, Delft University of Technology

Abstract

A seismic survey acquired by the petroleum company Wintershall has been used for this study in order to characterize the fault and fractures present in the area using the latest seismic attribute techniques. With the use of the software OpendTect from dGB Earth Sciences and a methodology developed by (Jaglan Hardeep, 2016) and (Qayyum F, 2015) is used in order to apply the latest seismic attributes to enhance the detailed characterization of fault and fractures from a seismic survey acquired by the petroleum company Wintershall over the F10 block in the Dutch North Sea, offshore The Netherlands.

The methodology to enhance faults and fracture is divided in three phases based on their objective. The first section of the methodology focuses on conditioning the data, to generate a volume that honors the dip and azimuth of the overall geological structures. This volume is defined as the Steering cube and is the framework for the application of the latest seismic attributes. The second phase is the application of the seismic attributes to enhance the faults and fractures encountered in the targeted horizons belonging to the lithostratigraphic groups. The third and last section is to manually interpret the faults and fractures to obtain length scales and orientation of the geologic structures characterized. Allowing to obtain fault and fracture network characteristics in terms of frequency, orientation and length scale. Finally, this study aims to provide recommendations on how seismic attributes can provide indications of sub seismic fractures.

Key words: seismic attributes, faults and fractures, length scale, sub seismic

Acknowledgements

To the Faculty of Civil Engineering and Geosciences from the Technical University of Delft my alma mater.For letting me allowing me process of studying my master program of Petroleum Engineering and Earth Sciences, by far the most challenging, unique and fulfilling experience I have lived. I would like to thank and recognize my master thesis supervisor prof. Giovanni Bertotti for having the patience and the knowledge to guide me along all this project and in the culmination of this period as a master student in Petroleum Engineering and Earth Sciences with the specialization in Reservoir Geology, without him and his broad experience this project would've never been possible. Special thanks to the company Wintershall for providing the high quality seismic survey from the North Sea, without this information this study would have not been possible. To dGB Earth Sciences for providing the full packages software and license. Special thanks to Farrukh Qayyum from for all his time and knowledge invested to provide his support to complete this project. Dr. Nico Hardebol for sharing his knowledge along the project and guidance. To professor Allard W. Martinius and Dr.ir. Guy Drijkoningen for being part of the committee. To my father, my mother and brother, to my family who have been supporting me in all the decisions that I have taken personally and professionally, for their unconditional love and support, for their understanding that is proven every day disregarding the distance, I will be forever in debt with you. To all my colleagues in the master program that believed in me and supported me while studying for every challenge encountered during this years, these challenging times made us more united and stronger for the coming future, you will always count with me. To the national Council of Science and Technology from Mexico for all the economic and moral support, for believing in a better more inclusive country where everyone can have access to a better and fulfilling scientific education. Without their support and comprehension this project would´ve never been possible.

Table of Contents

Table of Figures

List of Tables

1
Introduction

The impact that faults and fractures have in extraction industries like Geothermal energy, Petroleum industry and Mining industry is unquestionable and of great importance. The correct delineation of faults and fractures can constrain the viability of the projects developed in the mentioned industries. Depending on the type of operations, fault and fracture networks can generate benefits for the projects developed in this industries or act in detriment of them (Oppermann, 2012). In the Petroleum industry a correct characterization can provide positive effects, for example in naturally fractured reservoirs like the ones found in the Mexico, faults and fractures can become conduits for the hydrocarbon production, a correct characterization of the fault and fracture network can be included in production and optimization operations enhancing the project economic benefits and viability (Verduzco, 2010). As well a good characterization of the fault and fracture network can deliver optimization plans for drilling operations (Petukhov A.V., 2015).On the other hand, a poor understanding of the characteristics of the faults and fractures can evolve into catastrophic problems in drilling and production operations. (Oppermann, 2012)

With the advantages that computer machine has brought, new methodologies have evolved in the last decade that allow geoscientist to manipulate seismic surveys in a more robust way and to develop better fault extraction methods, as well to apply the most advanced seismic attributes in order to gain more valuable information that is contained in the seismic (Opperman, 2012).

The aim of the study is the application of the methodology developed by (Jaglan Hardeep, 2016) and (Qayyum F, 2015) to generate seismic attributes for an improved fault and fracture characterization with the latest seismic attributes techniques. This methodology allows to generated fault and fractures measurements based on the seismic information, rather than just creating a measurement of faults and fractures based only on interpretation of the faults and fractures with a manual interpretation.

This study aims to manipulate a seismic survey acquired in the Dutch North Sea offshore the Netherlands over the quadrant F10. With the application of the methodology proposed by (Jaglan Hardeep, 2016) and the use of the software OpendTect this study generates the most ideal framework for manual fault and fracture mapping hence marking the preamble for the generation of deterministic fault and fracture networks.

Problem Statement

Usually large-scale faults above 30 meters of throw displacement with lengths ranging 100 to thousands of meters are identified in seismic surveys without the application of seismic attributes or any enhancement. Due to the relation that exist between fault length and fault displacement, when the fault length decreases the throw also tends to decrease (Seon, 2004). Due to this relation faults become more difficult to be interpreted form normal seismic in vertical and horizontal sections, where the displacement and the length become sub visual to the interpreter eyes and enter in the sub seismic category. The faults are categorized as sub visual and sub seismic faults due to the fact that normal seismic surveys present great difficulties for their visualization by the interpreter eyes and also because the displacement of the throw is under 30m, which is defined as seismic resolution, respectively. Geoscientists in their attempt to interpret faults and fractures manually typically tend to under sample these faults as the confidence to visually interpret them is reduced due to the fact that the fault throw decreases (Oppermann, 2012). In today's industry the standard seismic surveys are underutilized and the methodologies to extract the faults provide less number of faults and fractures that the ones that really exist. Geoscientist need to interpret faults and fractures that fall in the category of sub visual and sub seismic resolution.

Research Goals

The research goal is to compare the faults and fractures present under the different regional tectonics encountered in the study area by analyzing and comparing their fault network and their length scaling rules. The study focuses in analyzing Jurassic And Cretaceous horizons that have been affected by various tectonic events. This study aims to determine how the seismic attributes can allow us to characterize with more accuracy, precision and confidence the faults and fractures present in each horizon, as well this study aims to provide recommendations on how seismic attributes can be indicative of sub seismic fractures. Implementing and understating the response of the attributes that improves the visualization, then delineation and extraction of faults at the highest possible resolution, using the latest seismic attributes. Subsequently create with the methodology proposed by (Jaglan Hardeep, 2016) and (Qayyum F, 2015) a better, more suitable framework for the manual interpretation of faults and fractures, hence creating a discrete fault network on an enhanced seismic volume. With the use of OpendTect, this study attempts to identify faults that with standard methods where no attributes are used would not be visualized and identified. This study aims to apply the latest seismic attributes to generate the most ideal framework to interpret and define sharper faults, this can be used as guidance the generation of a deterministic fault network.

Proposed Strategy

With the aid of OpendTect and following a methodology proposed by (Jaglan Hardeep, 2016) and (Qayyum F, 2015), where the latest seismic attributes will be applied to targeted horizons that belong to the Jurassic and Cretaceous periods, the horizons are present in the study area of the F10 block, offshore The Netherlands. The methodology followed focuses on conditioning the seismic by removing the unwanted noise, creating a volume that honors the dip of the overall geological structures in the basis of a steering cube. This generates the ideal volume to apply the latest attributes and to enhance the fault and fracture detection. Manually interpret the faults and fractures to extract length scales and orientation of the fault network. Finally, with the evaluation of the length and orientation, provide length scale rules and compare the for each network. This strategy will allow us to obtain the most ideal fault and fracture network for each horizon and understand the objective of manually interpreting the characteristics of the faults and orientations is to generate a discrete fault network on the Scruff, Rijnland, Chalk and North Sea group horizons based on observations and analysis rather than assumptions.

2

Literature Review

2.1 Geological Background

In this chapter the Geology related to the structural development of the Netherlands is enclosed. Focus is made on the most prominent tectonic phases that developed the structural elements important for this study.

2.1.1 Geology and tectonics

The studied area is located in the most Southern part of the Dutch North Sea basin. This basin is mainly formed by a range of platforms, sub-basins and highs, that are result of several tectonic phases that range from the Early Paleozoic to the Tertiary (J. de Jager, 2007). The Dutch North Sea basin experienced a wide range of geological events that were governed by alternating compressional and extensional tectonic phases affecting the area, result of rifting pulses during the Triassic to the Jurassic that generated a very complex and irregular Geology. Figure 1 illustrates the most prominent structural elements for the region of interest, making emphasis in the Dutch Central Graben, the Step Graben and the Cleaver Bank high platform (J. de Jager, 2007).The tectonic geological history of the Netherlands can be divided into three main tectonic phases:

i) Variscan orogeneses occurred in the Paleozoic, during the Hercynian, orogenic cycle fold belts were created in Africa, North America and Europe (Ziegler, 1990). The Caledonia Orogeny started the collision between three microcontinents, Baltica, Avalonia and Laurentia. Eventually large mountains systems were created due to the collision of Gondwana an Laurussia (M.C. Geluk, 2007)

The Variscan Orogeny took place Carboniferous it began with the amalgamation of the continents Laurussia and Gondwana resulting in the formation of the super continent Pangea, which was completed at the end of the Permian. This created a obstruction of the Rheic Ocean, and then developed the Rheno-Hercynian fold and thrust belts. The remainder of the Permian is as well defined as a period of relative tectonic calm, and with a long wavelength of thermal subsidence accentuated by minor tectonic pulses (M.C. Geluk, 2007).Is in this period when large and widespread deposition of the Zechstein evaporites and carbonates was established due to restricted marine conditions in that period.

ii) Mesozoic rifting was associated to the separation of the super continent Pangea. The Pangea continent started to break up in the Triassic, as a consequence the Central Graben system in the North began to form (figure 1). The faulted system is characterized for being formed essentially with three arms the Central Graben in the South, The Viking Graben in the North and the Moray Firth Basin in the west. In this period, extension took place with main direction east-west (Zanella E., 2003), causing faulting in the Central Graben and the Step Graben with a north-south trend figure 1. During the Middle Jurassic extension reached the Southern North Sea (J. de Jager, 2007), in this period also uplift took place and centered at the triple junction of the three rift segments and led to a formation of a dome named Central North Sea Rift Dome (Ziegler, 1990) , this had as a result erosion of a wide spread area that extended to this studied location, sediments were only preserved in the graben area. Subsidence resumed during the Late Jurassic and sediments deposited again outside the graben. Continental break up of Pangea was reached in the North Atlantic in the Late Jurassic, this characterizes the end of the period of extension. Because of this finished rift period, and because the rift did not completed it was defined as a failed rift system (Ziegler, 1990).

iii) Alpine inversion developed by the collision of Africa and Eurasia causing widespread inversion during the Late Cretaceous and Early Tertiary. During the development of the Alpine orogenic system a considerable number of inversion events developed during the Late Cretaceous and the Paleogene (J. de Jager, 2007).This inversion events had distal effects significantly affecting the Southern North Sea area lifting the Mesozoic basins causing erosion above the Dutch Central Graben and the Step Graben (Jager, 2003).

2.2 Structural elements

In this section genesis of the most prominent structural elements are explained, focusing on the Dutch Central Graben Step graben, and the Clever Bank High due to the fact as they are part of the seismic survey. (Figure 1)

2.2.1 Dutch Central Graben

This prominent structure has been described as a complex area that evolved because of an extensional rifting regime (Wride, 1995). This structural feature is defined to have been developed mainly during the Triassic, Jurassic and to the Early Cretaceous. Location of the Dutch Central Graben is illustrated in figure 1. The Central Graben development was controlled by previous fault lineaments which constrained important features for the formation of the graben. The main fault trends that have been identified are i) NW-SE trend, result of the Variscan fault belt (I. D. Bartholomew, 1993) ii) N-S fault trend that is attributed to the early Caledonian and iii) E-W trend originated in the pre-Variscan to Carboniferous extension. Studies state that the most dominant structural development of the Central Graben was a combination of extensional rifting modified by halokinesis and inversion during the late Jurassic (Wride, 1995). Structuration of great part of the Dutch central Graben occurred in several rifting phases recognized as the Permian rift, the Triassic to Jurassic rift and the major Upper Jurassic until the Tertiary phase deformation (Wride, 1995) during the Mid Kimerian and also the Late Kimerian rifting phases. Inversion during the Cretaceous and Tertiary affected the Dutch Central Graben, although these effects decrease towards the North.

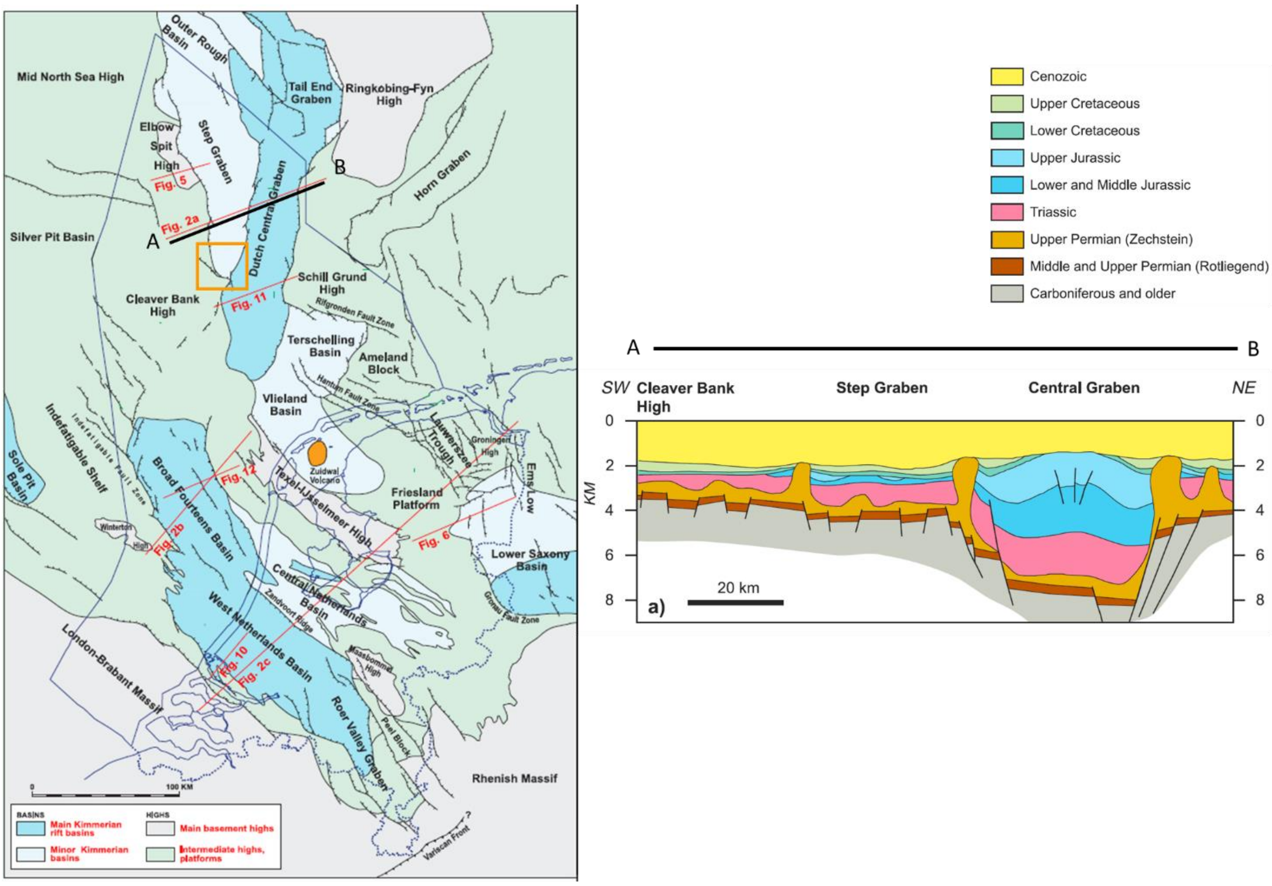

Figure 1. Structural Elements of the Dutch North Sea, area of interest of the F10.In orange the location of the seismic survey over the F10 Block. 1a)Regional cross-section of Dutch Offshore Block (J. de Jager, 2007)

2.2.2 Step Graben

Studies have determined that the Step graben formed along with the Dutch Central Graben during early Carboniferous (J. de Jager, 2007) see location of Step Graben in figure 1. Activity after the Carboniferous has been recorded, the main and most prominent phase happened during the Triassic and Jurassic, with some pulses up to the Cretaceous characterized the period of the breakup of Pangea. The Step Graben is characterized to be formed along the north-south faults that were caused by the East-West extensional regime. The Step graben has been defined as minor graben or terrace, of lows and troughs formed mainly by the Outer Step Trough, the Step Low and the Step Trough, with significant Triassic and Cretaceous sediments and in some parts separated by the highs. The Step Graben is bounded in the east by the Dutch Central Graben and in the wet by the Clever Bank high in the east and the Elbow Spit Platform in the East.

2.2.3 Cleaver Bank High

The first activity that has been recorded for the Cleaver Bank High developed in the Variscan Foreland as a cause of the wrench tectonics regime during the Carboniferous (Ziegler, 1990). The most prominent tectonic pulses after the Carboniferous that affected this structure is the Kimmerian rifting phase that took place in the Late Triassic due to the Pangea break up of until the Jurassic. Finally, this structure was affected as well by the Pyrenean and Savian pulses of the Paleogene that are related to the Alpine inversion.

2.3 Lithostratigraphic Groups

In this section the important lithostratigraphic for this study are described as they are targeted for the fault and fracture analysis. The lithostratigraphic groups are the Scruff, Rijnland, Chalk and North Sea Group. The target lithostratigraphic groups are represented in the study as horizons where the seismic attributes are calculated.

2.3.1 Zechstein Group.

The deposition of the Zechstein was characterized by a complex interplay of transgressions coming from the Arctic and with evaporation taking place in the South Permian basin. The Zechstein group is mainly formed by five evaporite cycles and is characterized to be a complex sequence of sediments, mainly formed of shallow and deep water evaporitic facies where basinal halites and shelf carbonates account for the most. This stratigraphic sequence lies on top of the Lower Permian Rotliegend sandstones. The Zechstein Group deposited in the Southern Permian Basin, which was separated in the E-W Mid North Sea Ringkobing Fyn High (figure 1). Thicknesses ranging from 1500 to 2000 can be recognized in the deepest parts of the South Permian Basin (Ziegler, 1990). The Zechstein Group is stratigraphically constrained between the copper shale Member at the base and the Zechstein Upper claystone formation (J.H. ten Veen, 2012).In parts where the Zechstein group forms diapirs, walls or pillows the thickness can exceed the 8000 meters.

2.3.2 Scruff Group

This formation was deposited in the Jurassic, the age ranges from Late Oxfordian to Ryazanian it consists mainly of marine and bituminous claystones containing some intercalations of carbonate beds, as well glauconitic, argillaceous, fine to coarse grained sandstones (J. de Jager, 2007). The distribution of the Scruff group has been recorded and accounted to areas in the Dutch Central Graben. Within the F quadrant great variations of thicknesses are recognizable and are accounted to strong differential subsidence and erosion during the Subhercynian and Laramide inversion phase.

2.3.3 Rijnland Group

This deposit corresponds to the late Jurassic and Early Cretaceous specifically to Ryazanian or Valanginian to Albanian. The lithology of the Rijnland group is mainly comprised to be deposits containing argillaceous and marly, siltstones and glauconitic sandstones. Further divisions of the Rijnland group encompass the Vlieland Sandstone, Vlieland Claystone and the Holland Formation. Sedimentation occurred in wide area of the Netherlands, but not in the Texel-Ijsselmeer High and Southern part of the Netherlands (J. de Jager, 2007). Due to inversion it was eroded in some Jurassic and Cretaceous basins. In the Lower Cretaceous a large number of depressions overlying the Jurassic Grabens were filled due to a transgression. Depocenters were areas of thicker deposition and were separated into discrete basins that lie between the main fault systems.

2.3.4 Chalk Group

The Chalk Group deposited during the late Cretaceous and Early Tertiary in the North Sea basin. (Bonnet, et al., 2001)This group is present over most parts of the Netherlands and in the offshore area. It is locally absent in the Dutch Central Graben due to erosion that took place during the Late Cretaceous and earliest Tertiary. The most prominent divisions in the Dutch sector are the Ekofisk Formation, the Ommelanden Formation and the Texel Formation. The economic importance of the Cretaceous deposits is of great relevance as many oil and gas fields have been found in the North Sea. The two major compressional phases occurred namely the Sub-Hercynian phase, began in the Early Turonian through the Early Maastrichtian, the second compressional is called the Laramide. This phase took place during Danian in the Early Tertiary (Ziegler, 1990).The deposition of the Chalk Group finished with the Alpine continental convergence, as a result of this orogeny large influx of eroded material deposited in the ocean eliminating the ideal conditions for chalk to be formed. The sediments of the Cretaceous Group are characterized to be sediments with white or cream to grey, fine grained, bioclastic limestones and marly limestones (J. de Jager, 2007).

2.3.5 North Sea Group

The North Sea group is mainly conformed by post- Oligocene sediments, it overlies the Chalk group and also older Mesozoic strata. It is divided into the Lower, Middle and Upper North Sea group. It is formed by alternations of sands and clays in the direction of the Southern margin of the North Sea Basin (J. de Jager, 2007). The group occurs in the vast area of the Netherlands and shows high variations due to syn-sedimentary block faulting, halokinesis and erosion.

2.4 Halokinesis

The type of structures encountered in the study area are a result of two phases that affected the salt tectonics, the phases occurred in the Late Triassic and the Tertiary. During the Triassic phase, a large number of salt pillows and isolated diapirs formed (Wride, 1995), the second phase is mainly represented by period of formation of diapirs in the area known as the Salt Dome province and belongs to the Tertiary phase.

2.4.1 Faults and salt structures relationship

A set of large scale structures are developed during the extensional regime and presence of salt layers. These structures illustrate the large-scale faulting models that can be found in the area where salt and extensional regime occurred. The structures have been analyzed and have been encountered in the Dutch North Sea, offshore the Netherlands. This model states that structural style that dominates the initiation of the rift event is also dependent on the amount of salt deposited previous the rift (Oliver B. Duffy, 2013). The idea that salt structures were only, buoyancy-driven piercing structures has evolved and now has converted it into a phenomenon that associates the structures with the main extension regime that occurred in the formation of grabens. In order to systematically analyze and distinguish the faults associated to salt, three main categories have been studied and can be distinguished in following categories (figure 2).

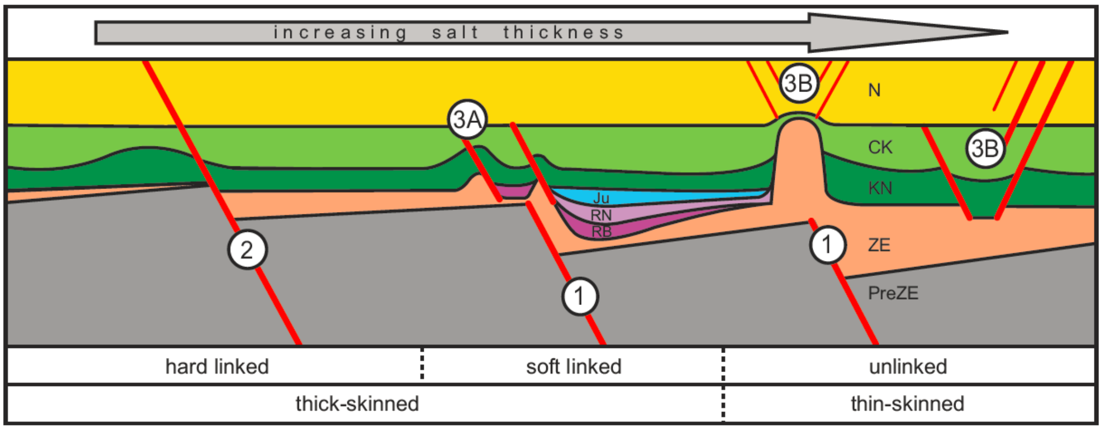

Figure 2. Faults and Salt structure relationships (J.H. ten Veen, 2012)

1)Unlinked Thin skinned. In this case no relation exists linking the fault above and below the thick salt layer as they are decoupled. This system is termed unlinked as no spatial relation of the faulting between the overburden and beneath the salt. Figure 2

2) Soft Linked Thin Skinned. This system is characterized for having an intermediate level of salt. Faults from the overburden and below the salt layer are spatially linked and can demonstrate a lateral offset mostly in the footwall. This system may evolve to a hard-linked system if the fault that develops in the over burden aligns to the fault beneath the salt layer (Stewart, 2007).Reactivation of unlinked faults from a thin-skinned system can also evolve into thick skinned system.

3)Hard Linked System. Faults. This is characterized by faults that are present above and below the salt layer, meaning the fault is connected along the salt. From the systems this one present the thinnest and the lowest amount of salt (J.H. ten Veen, 2012).

In the study area the large-scale model that has been identified is the soft linked, thinned skinned system. These large-scale features where encountered in the seismic volume proposed. The scale of this features is visualized directly in seismic without enhancement. As part of this study this fault models are mentioned to see if a relationship is found with smaller scale faults and fractures that are interpreted and see if there is a relationship between them. Figure 3 shows the type of model encountered in area that belong to the F10 Block where the seismic survey was acquired.

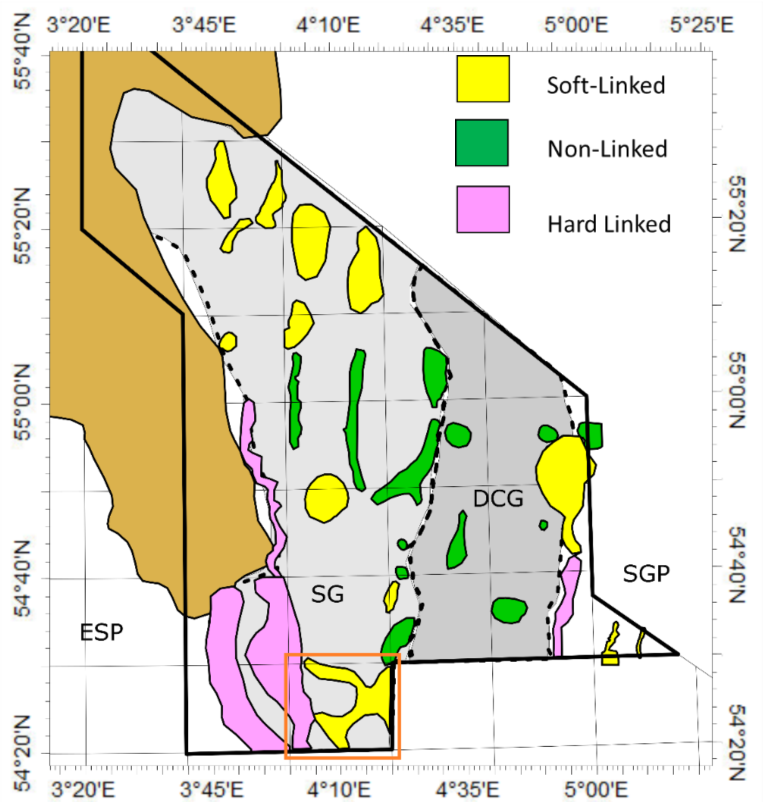

Figure 3. Location of the F10 block enclosed in orange square.Map shows the characteristics of the large scale faulting system of the salt structures offshore the Netherlands.

The salt structures developed in offshore the Netherlands were caused due to the mobilization of the Zechstein Group and tectonic phases. This mechanism has been systematically approached by different authors. Van Winden proposed a logical discrimination of salt structures based the next characteristics. 1) Orientations and Dimensions 2) Faults 3) Associated stratigraphic relations and 4) Data and Location (Winden, 2015).

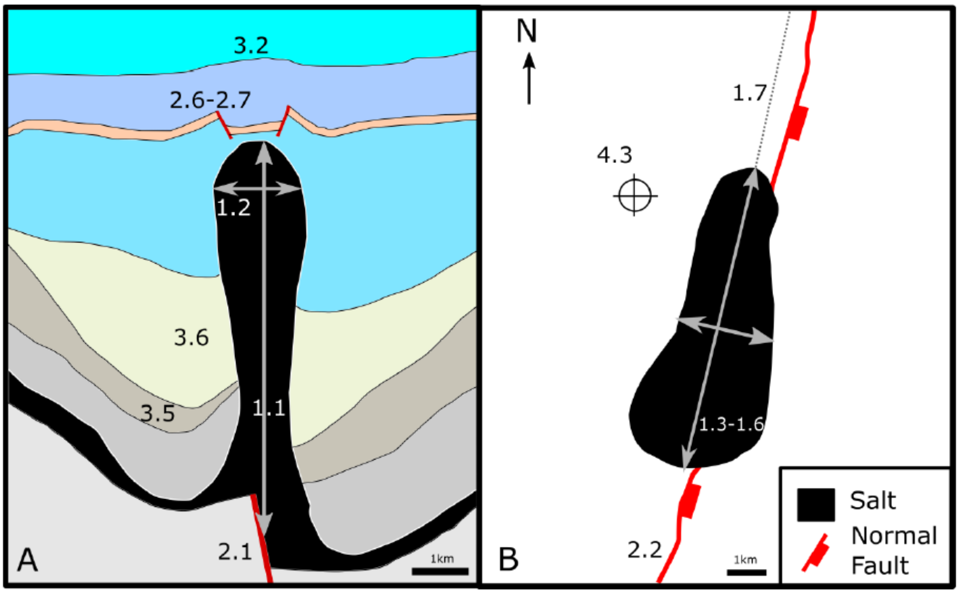

Figure 4. Schematic of the salt structure showing the dimensions analized in A)Verical view of the salt structure B)Top view o the salt stucture sketch.1.1: Height fromZechstein, 1.2: Maximum width,1.3-1.4:Length and with of the salt structure,1.5:Elliptical ratio, 1.6:Shape type,1.7:Orientation, 2.1 Fault type below the salt structure, 2.2:Orientation of the sub salt fault 2.6-2.7 Fault type above the salt structure.

Salt structures can be characterized based on dimensions and orientations, without focusing on the other categories and taking only the category of dimension and orientations, the salt structure encountered in the F10 Block is determined to be a salt wall (Winden, 2015). Van Winden proposed a method that differentiates salt structures from being pillows, walls and diapirs. The methodology is based on the measurement of the maximum angle that the top of the salt structure with respect of the horizontal line at the base of the structure as in figure 4.

Salt Structure definition	Angle of Flanks	Elliptical ratio	Piercing
Pillow subtle	< 30 º	-	No
Pillow pronounced	< 75 º	-	No
Diapir	> 75 º	< 4	Yes
Wall	< 75 º	> 4	Yes

Table 1.Characteristics of salt structures based on the dimension charcateristic and angle with respect to the base of the Zechstein group.

The distribution of salt structures in the Dutch North Sea Offshore the Netherlands can be seen in figure 5. These structures were characterized and analyzed to generate and differentiate the salt structures from being salt pillows, salt walls, and diapirs. The study area of the F10 Block is enclosed in the red square, this image shows the structures encountered for this study are determined to be salt walls. Pronounced pillows are in light purple, and in red are the salt wall structures that are found in the study area.

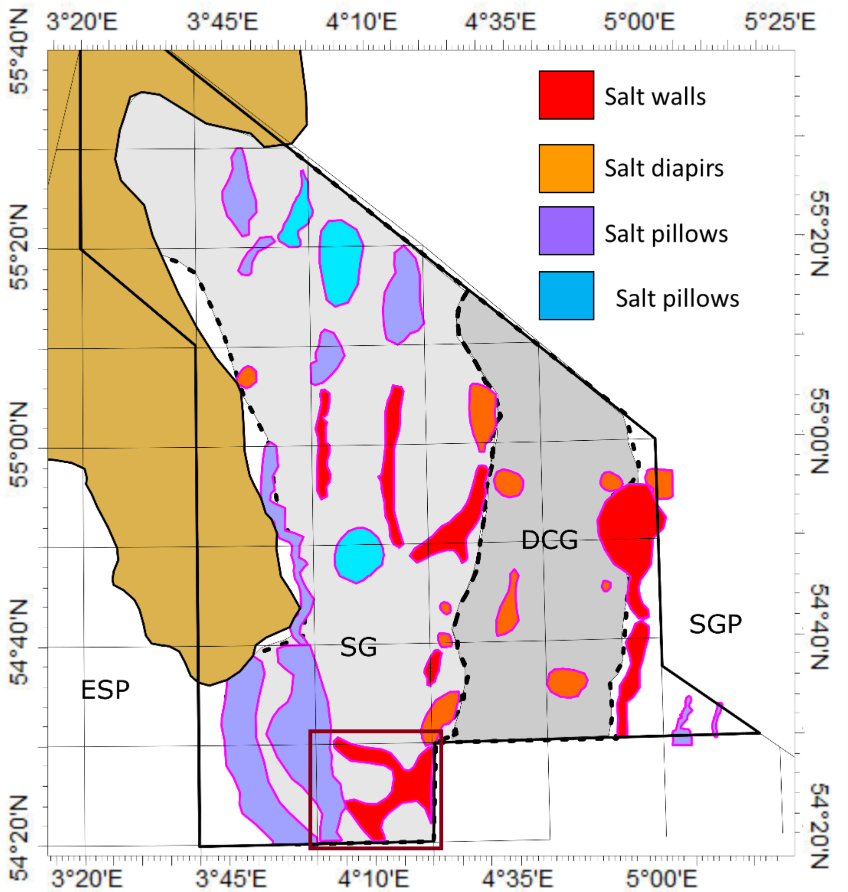

Figure 5. Distribution of salt structures Offshore the Netherlands.Location of the F10 block higlighted inside the red box.

3

Data set

For this project the seismic survey acquired by Wintershall over the block F10 offshore the Netherlands is used (figure 6). The survey comprises 827 in lines and 2154 crosslines. In line number (100 to 927) crossline ranging in the numbers of (193 to 2347) over the F10 Block of the Dutch offshore. The prospect area is situated in the most southern part of the Step Graben, where it encounters the Clever Bank High, and the Dutch Central Graben (figure 1). The area covered by the survey is 557.74 km^2 and was acquired in a configuration of 25 meters by 12.5 meters for the bin size in the in line and cross line respectively. The In lines are oriented 269.05 degrees from the North.

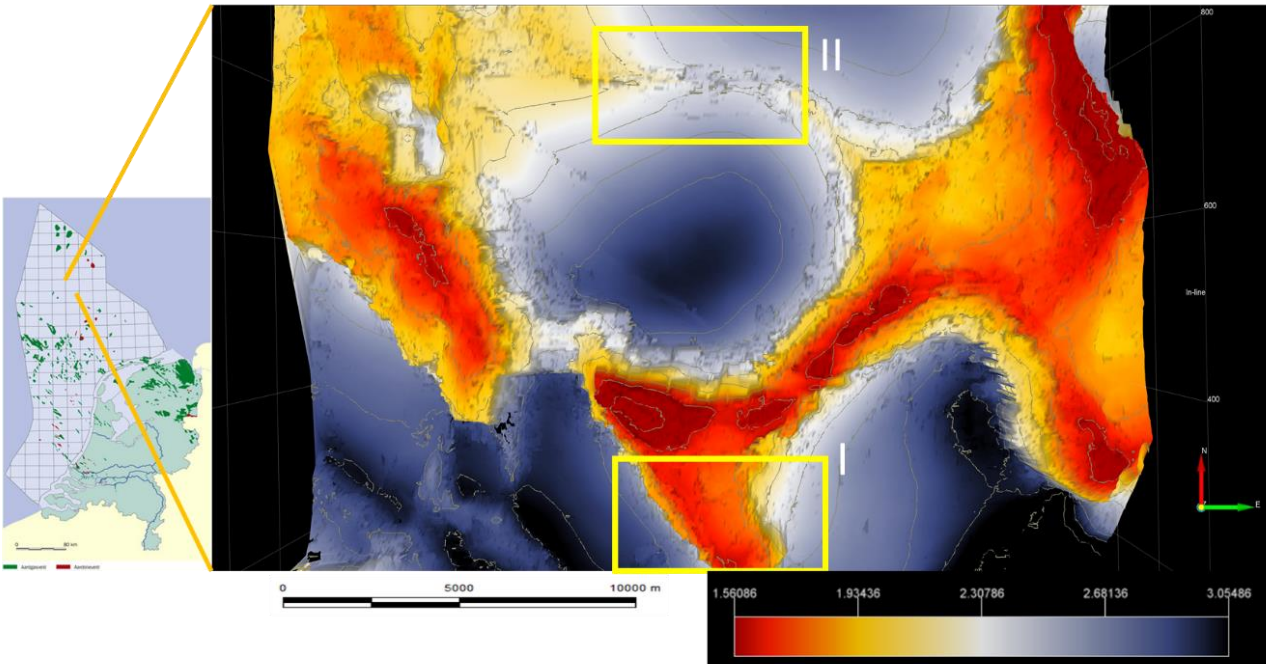

Figure 6. Location of the Cropped Steering cubes I and Steering Cube II. Locaion of the F10 Block Offshore the Netherlands .

3.1.1 Determination of the study domain

For this study, two areas have been analyzed, the first seismic volume to which will be referred to as Steering Cube I is an area of the original seismic survey and is defined as a cropped seismic volume constrained by the in lines (100 to 250) and crosslines (933-1448) respectively, with the in lines oriented 269.05 degrees from North and the total area comprising 24.137 km^2 is proposed. Figure 6 Shows the top of the Zechstein horizon group and the location of the Steering Cubes offshore the Netherlands.

In this area the deformation of the horizon is considered to be high, the 4 horizons are present, allowing to make comparisons of the resulting fracture network and scaling rules of each horizon with respect to each other, allowing to understand if there are differences or similarities between them regarding the origin of the faults and fractures and determine if there is any relation with the large-scale features. As well, another reason to select this area is to be able to analyze and describe the targeted formations by describing the lateral changes, as well to analyze if there is a relation between the salt structures, as the main drivers of the origin of the faults and fractures.

The Second which is referred to Steering Cube II is in the same F10 Block and is constrained by the in lines (721 to 927) and cross lines (1500 to 1041), as well oriented 269.05 degrees from the North and comprises a area of 29.235 km^2 . Figure 6 shows the location of the Steering Cube II.

The second Steering cube is located most Northern part of the F10 Block (figure 6). The reason to choose this study area is the characteristic fault network encountered, this selection allowed to make comparison of the faults with different regional tectonics. This variation allows to study in accordance with the research goals, the targeted horizons and compare the faults and fractures characteristics in different tectonic domains, analyze if there are differences as well their length scale rules between them and in frequency. For the second Steering Cube the deformation is determined to be less deformed than the first Steering Cube hence allowing to analyze the faults and fractures in different domains and make comparisons between them.

4

Methodology

For the present study the methodology followed is described in figure 7 and provides an ideal workflow for the application of the seismic attributes to achieve the fault and fracture characterization (Jaglan Hardeep, 2016). The methodology encompasses two main aspects i) the conditioning of seismic data enclosed in the proposed domain to obtain the dip and azimuth of the overall structure, remove noise and acquisition footprints, pitfalls that seismic surveys inherently contain. ii) calculate the seismic attributes in order to generate the most deal framework for the fault and fracture characterization. Finally, with the interpreted faults and fractures in the ideal framework. A third phase is to iii) determine and quantify the length an orientation of the faults and fractures in order to provide length scale characteristics and to analyze the fault and fracture network in frequency, length and topology. The results are then analyzed to compare their length scaling rules for the faults and fractures interpreted in the horizons. Finally provide information on how seismic attributes can be indicative of sub seismic faults and fractures.

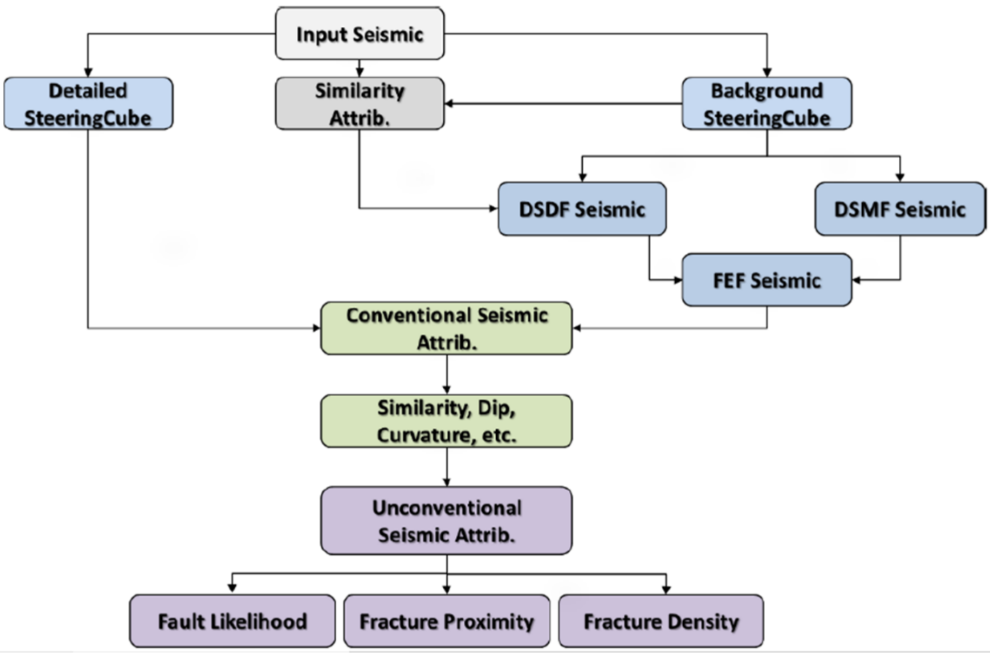

Figure 7. Methodology proposed modified from (Jaglan Hardeep, 2016).Flowchart for application of the conventional and unconventional seismic attributes

4.1 Conditioning the data

The conventional seismic data usually contains noise and pitfalls due to acquisition or incorrect processing, another reason is that geological features can be affected by acoustic disturbances that can veil their proper visualization. A systematical method to filter the seismic and remove the random noise from the seismic data allows to improve and enhance the lateral continuity of seismic events and allows to delineate sharper faults and fractures.

4.1.1 Extracting dip and azimuth trough Steering Cube

The dip computation marks the framework to further filter the post- stack seismic and to generate geometrical seismic attributes, the seismic dip is an attribute itself and it is used to correct the structurally oriented filters. The dip of the seismic is an attribute that allows to guide the analysis of further attributes like similarity, hence the importance of this calculated volume that is named as a Steering Cube. The dip of this post stack seismic volume can be calculated trough three methods i) Amplitude based ii) Phased based iii) Amplitude-frequency based (Marfurt, 2007).In this project OpendTect is used and calculates the dip trough the Phased- based method using of BG fast algorithm. Different steering cubes can be created depending on their objective that is pursued, this are Background steering cube and Detailed Steering Cube (Qayyum F, 2015).

4.1.2 Background Steering Cube

The strongly filtered Background Steering cube allows to determine the overall trend of the large-scale dip trends and the seismic reflections. This is a strongly filtered cube that allows to determine the trend of the large dip and is used for the further analysis of structural oriented processing (Qayyum F, 2015).The Background steering cube mostly contains the information of the primary geologic structure. It is used mainly to accentuate the overall geologic structure as well to calculate the multi-trace attributes like similarity. This cube is used for the evaluation of Dip Steered Median Filter and Dip steered diffusion filter. Inputs that eventually are used for the creation of the Fault Enhancement Filter.

4.1.3 Detailed Steering cube

A less filtered cube is defined as Detailed Steering cube and allows to further calculate more localized characteristics for local dips of seismic reflectors. This cube preserves the small variations on the seismic reflection and contains the information of the faults or flexures from the subtlest geological features (Qayyum F, 2015). It is used to maintain the detailed features for example in the curvature attribute in order to accentuate the flexures on the horizons.

4.2 Structural oriented filters

This method creates an enhanced volume that allows the interpretation of faults and fractures by smoothing the seismic reflections, enhancing the edges of the seismic reflector and preserving the characteristics of the structure. (Jaglan Hardeep, 2016). The enhancement of the signal quality is achieved by suppressing the random noise that is contained in the signal. and it is performed by processing and conditioning the seismic data in a routine way. The method proposes three steps i) create an improvement in the lateral continuity of the seismic reflectors, achieved with the Dip Steered Median Filter, ii)improving the position of the fault, using the dip steered Diffusion Filter and last, iii) merge previous two steps in order to create a logical statement to produce a Fault enhanced seismic data (Qayyum F, 2015).

4.2.1 Dip Steered Median Filter

This filter is applied using the background steering cube which contains the large-scale dip trends (Marfurt, 2007). The statistical filter smooths the seismic volume, preserving and improving the lateral continuity of seismic reflector and removing the background noise by using the median statistics of the seismic amplitudes and following the seismic dips (Qayyum F, 2015). This filter can smooth too much the discontinuous features like faults and fractures, this is dependent on the size of the fault zone. If the fault zone smaller than the mean is smoothed out hence another filter named Dip Steered Diffusion Filter is applied. This Filter is mostly used for the to remove the noise for the seismic.

4.2.2 Dip Steered Diffusion Filter

This is defined in the routine as the intermediate step that takes the advantage of the diffuse character of the signal close to a fault. The Dip Steered Diffusion Filter utilizes the diffuse characteristic near to the fault and evaluates the seismic data in a dip steered circle, it replaces the diffused seismic traces near to the fault and replaces them with the better quality seismic traces, resulting in sharper faults (Jaglan Hardeep, 2016). The Dip Steered Diffusion filter is mainly used to make sharper faults by enhances the diffusion in the proximity of the fault. This filter is the input for the calculation of the Fault Enhancement filter.

4.2.3 Fault Enhancement Filter

The final stage of the method to obtain structural oriented filters is achieved by combining previous two logical filters. The DSMF and DSDF which are systematically applied in conjunction to obtain a geometrical seismic attribute named Fault Enhancement Filter and calculate with this the similarity. The Fault Enhancement Filter attribute uses a defined threshold value in order to systematically apply previous filters DSMF and DSDF. As FEF is computed analyzes the similarity attribute if it is above the threshold proposed it applies the DSMF meaning that the lateral correlation exists (Qayyum F, 2015). If the similarity is computed and is below the threshold value it uses the DSDF to enhance the faults that can be present.

4.3 Seismic attributes

This is second part of the methodology followed (figure 7), where the creation of the geometrical attributes take place on the targeted horizons. The method relies on applying the geometrical attributes systematically to image the complex geological features encountered in the area of interest. The attributes allow us to extract the most detailed geological features. The attributes are applied in a sequential order, to enhance the characterization of faults and fractures of the Scruff, Rijnland, Chalk, and North Sea Group targets. The geometrical attributes applied are categorized as 1) conventional attributes and 2) unconventional attributes. Conventional attributes have been standard methods of great use in the industry and because of their common use, are termed this way. The term unconventional attributes refer to the fact that they are new techniques applied in the industry to obtain more information from the seismic data. With OpendTect the attributes are evaluated with specific entry parameters to test their result. The parameters were to calculate the attributes varied to obtain the best results temporarily this means are calculated either in one specific inline or crossline. Only when the result satisfies and honors the geological features, attributes are computed as volumes to build and to gain information of the whole seismic volume.

4.3.1 Conventional attributes

The term conventional is determined to this attribute as they are commonly used in the industry in order to enhance the seismic data to further characterization of geological features. Seismic attributes used in this study are characterized to be geometrical seismic attributes that follow the overall trend of the geologic features that are encountered in the subsurface.

4.3.2 Similarity

It analyzes the correlation of two trace-segments, it is a form of coherence defined by the distance in hyperspace between the vector of the segments (Paul de Groot, 2003), which is normalized to the sum of the length of the vectors. Similarity of the traces is estimated trough the reflection, computing the Euclidean distance between the amplitude vectors of the trace of the waveform (Tingdahl Kristofer M., 2005). It is namely a form of coherency that searches the correlation of the waveforms along a reflection (Paul de Groot, 2003).This similarity attribute is calculated since faults and fractures can be described as discontinuous reflection patterns that provide low response to similarity. For the purpose of evaluation of similarity equation 1 is described after (Tingdahl Kristofer M., 2005) to evaluate the dip steered similarity. This attribute allowed to discern faults and fractures as they are sensitive to the lateral position of the trace segment. The similarity is applied using the Fault Enhancement filter as an input, as well an evaluation of the similarity without steering is calculated in order to demonstrate the improvement that steering can generate. Dip steered similarity is evaluated in OpendTect after (Tingdahl Kristofer M., 2005) equation of similarity steered which is as follows:

$$S_{dip} = 1 - \frac{\left|a_{dip} - b_{dip}\right|}{\left|a_{dip}\right| + \left|b_{dip}\right|}$$

Where, $a_{dip} = \begin{bmatrix} u(x_A, y_A, t_A + t_1) \\ u(x_A, y_A, t_A + t_1 + dt) \\ \cdots \\ u(x_A, y_A, t_A + t_2 - dt) \\ u(x_A, y_A, t_A + t_2) \end{bmatrix}$ $, b_{dip} = \begin{bmatrix} u(x_B, y_B, t_B + t_1) \\ u(x_B, y_B, t_B + t_1 + dt) \\ \cdots \\ u(x_B, y_B, t_B + t_2 - dt) \\ u(x_B, y_B, t_B + t_2) \end{bmatrix}$

Where t_1 is the start time of comparison window, t_2 the relative stop time of the comparison of the second window, dt is the sampling interval. The dip steered times going from (x,y,t) are defined by t_A and t_B, respectively and are evaluated until the trace (x_A,y_A) and (x_B,y_B). As similarity is calculated values ranging form 0 to 1, are computed, if the trace segments are totally similar a similarity of 1 will be computed and if similarity is 0 the trace segments are completely different. (Tingdahl Kristofer M., 2005)

4.3.3 Curvature attributes

The different types of curvatures were created with the Background Steering Cube as an input, as this volume contains the dip of the volume in the inline and crossline direction of the overall geologic features. The curvature is an effective method to describe how much a surface of interest deviates from being a straight line (Roberts A. , 2001). The method of curvature attribute utilizes this concept to evaluate and to provide insight of discontinuous variations of geometrical deformation from being a straight line (Marfurt, 2007).A group of curvatures is used in order to evaluate geological features as anticlines or the upthrow part of the fault, for the latter the most positive curvature was used. A second method evaluates the most negative curvature providing idea of geological features like anticlines or the downthrown part of the fault. The different curvatures were evaluated as they provide great insight of faults and fractures. Images of the most Negative Curvature can be seen in figure 54 to 60 in Appendix included in this report

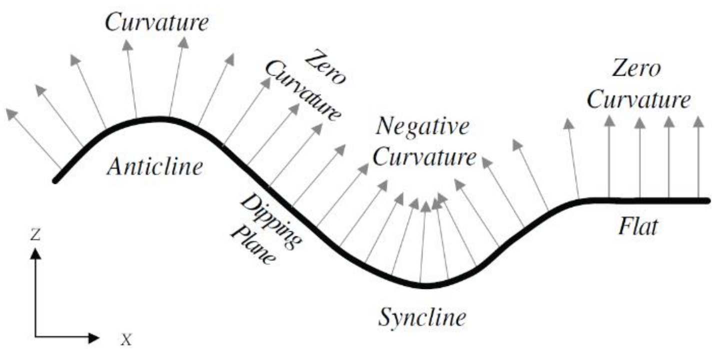

Figure 8. Curvature sketch after (Roberts A. , 2001) Showing the characteristics of the curvature analysys .

4.4 Unconventional Attributes

This are defined as unconventional attributes due to the fact that are of recent application in seismic interpretation for fault and fractures, OpendTect has developed three attributes that use as input the Fault Enhancement Filter enhancing the faults using the filters like Dip steered diffusion filter and Dip Steered Median Filter described in the previous chapters.

4.4.1 Thinned fault Likelihood

The thinned fault likelihood attribute is calculated with the Fault Enhancement Filter as an input which contains the information of dip in a volume. Through this volume of the dip and azimuth, it searches for the orientation of the minimum semblance along the tridimensional volumes. It is defined as a power of semblance (1- Semblance^n) (Qayyum F, 2015) delivering values in the between 1 and 0 showing (Jaglan Hardeep, 2016)the probability of the anomaly to be present. This attribute can generate faults and fractures that have non-geological dips and strikes due to its sensibility and due to the characteristic that these geological features represent the most likely, discontinuity possible (Hale, 2013) .

4.4.2 Fracture density

The fault density attribute is computed using the thinned fault likelihood volume and it allows to evaluate the area were fractures concentrate by calculating the ratio of a number of traces that are distinguished to be fractures with respect to the number of traces in a radio proposed (Qayyum F, 2015).This attribute allows to highlight the location of fractured areas in respect of a radius provided. In the case of the fracture density evaluated a radius of 100 meters was provided. It is useful for the analysis of fracking methodologies (Jaglan Hardeep, 2016).

4.4.3 Fracture Proximity

The method to evaluate this attribute is using the Thinned Fault Likelihood volume as an input volume. This unconventional attribute allows to characterize the fracture connectivity (Qayyum F, 2015). Utilizes the position of the trace that is identified as a fracture and evaluates the distance laterally. This attribute is determined by a threshold value, revealing the closeness of a particular sample from a fracture, as well the closeness between fractures. This attribute is used to visualize the connectivity of the fractured network (Jaglan Hardeep, 2016).

4.5 Interpreting fault and fractures.

The first part of the methodology is focused on conditioning the data for the structural analysis this is achieved by generating the Background Steering cube for the application of the Dip Steered Median Filter and the Dip Steered Diffusion filter. The next step is to apply the similarity attribute trough the Fault Enhancement Filter, this attribute provides the most suited framework for the manual interpretation of faults a and fractures. Manual interpretation is done over the horizons displaying the FEF Similarity and the Thinned Fault likelihood. These attributes were displayed in each inline and crossline and allowed to confirm and locate faults with low throw. This works for the validation of faults and fractures and to discriminate artifacts due to the fact that the attribute Thinned Fault likelihood is very sensitive and can deliver unrealistic or non-plausible features.

4.5.1 Fault length and orientation evaluation.

This process is based on exporting the faults and fractures that are characterized and manually interpreted with the aid of the tool OpendTect. Faults and fractures are manually picked with the tool named fault stick, this tool is a visual representation of the interpreted fault that contain location values in x, y and z coordinates. The values are obtained based on the interpreted faults that are found in the horizons of interest. Faults sticks are created in each horizon in order to manipulate and obtain values that describe the faults and fractures present in each horizon. The faults and fractures interpreted as fault sticks are then exported to determine the length scale characteristic and the orientation of the faults that to obtain length scale rules and network characteristics. After obtaining the most realistic and approximate fault delineation based on picking the faults and fractures, the set of fault sticks is exported as a csv file, csv stand for the term comma separated values. With the aid of excel the data is handle as in some cases hundreds of faults can be interpreted. In order to provide the orientation characteristics of the fault and fracture network present in each horizon a group of histograms are created to analyze if there is a relation between length and orientation, this way allowing to determine sets of faults and fractures that can be identified and visually described in rose diagrams are presented.

4.6 Length Scaling rules

Continuing with the analysis of the faults and fractures length, a power of law calculation is done with the aid of MATLAB to describe and to validate the length distribution of each horizon. The cumulative frequency is plotted against the length in a log-log scale. When the plot shows an acceptable straight line approximation the power of law can be accepted as a reasonable model to describe the fracture length distribution. (Bonnet, et al., 2001) The way the number of fractures decrease is explained by the equation: (Peacock D.C.P, Nixon C.W, Rotevatn A., Sanderson D.J., & Zuluaga, 2016)

$$N(l) = \alpha l^{-a} dl$$

$N(l)$ is defined as the number fracture lengths belonging to the interval determined as $[\, l, l + dl]$ for $dl \ll l, \alpha$ is a density constant and a is the exponent. As both axes follow a logarithmic progression the power of law exponent is $a-1$.Finally the exponent a is defined by the slope of the trend line.The line follows a negative slope due to the fact that the number of faults and fractures tend to increase as the length of the faults and fractures tend to decrease. With the use of the density distribution, $n(l)$ is determined to belong to the number of fractures $N(l)$, that correspond to an interval of bin size dl (Davy 1993). The density distribution is given by the equation

$$n(l) = \alpha l^{-a}$$

The cumulative distribution represents the number of faults and fractures that have a length higher than a determined l and belongs to the integral of the density distribution $n(l)$.

$$C(l) = \int_{l}^{l_{max}} n(l)dl$$

Where l_{max} is determined to be the greatest length characterized in the network.

To conclude if $n(l)$ is a power of law with an exponent a the cumulative distribution will be a power of law $l \ll l_{max}$ with the exponent to be $a-1$.

5
Strategy

In order to reach the objective of obtaining length scaling and network rules the cropped sections are analyzed in order to interpret the faults and fractures present in the horizons of interest. Figure 19 shows inline 192 of the Steering Cube 1, showing the Scruff formation is present only in small portion in the volume in the syncline, the Rijnland formation horizon is present in a portion of the volume. The Chalk and the North Sea group horizon are on top of the salt structure and can be found in all area of the Steering Cube I.

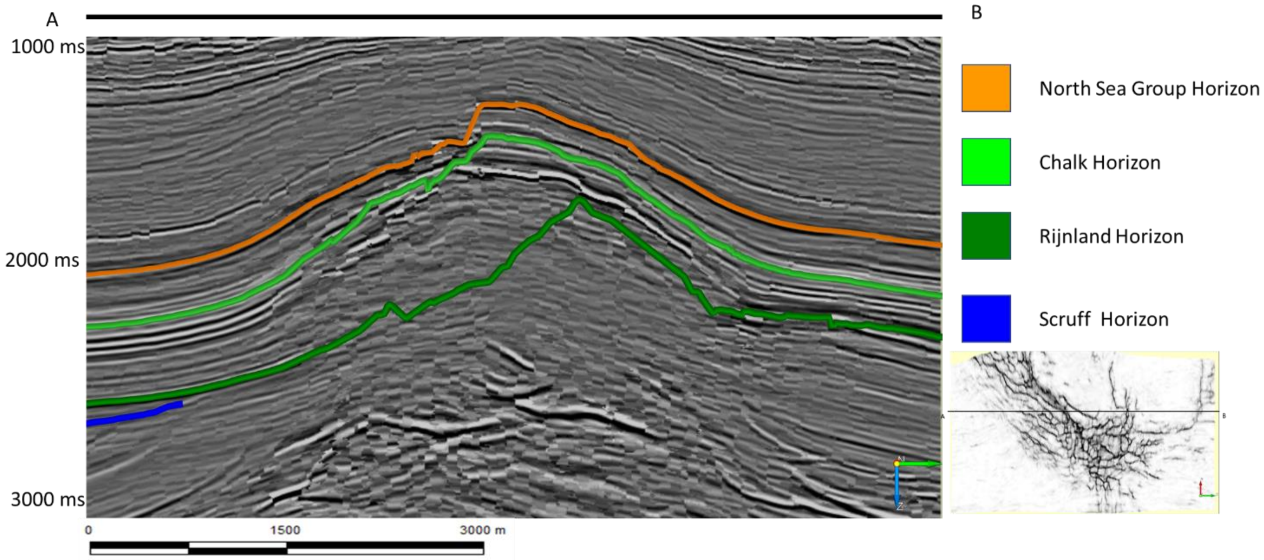

Figure 9.-Inline 192 from the steering cube 1.Showing the distribution of the target horizons.and location of the inline in the Steering cube I.

For the second Steering Cube the cross-line 1218 is shown in figure 10, the vertical section allows to visualize the targeted horizons in the area of interest. In this volume the horizons available are: Rijnland, Chalk and North Sea Group. The horizons are above the sault structure and were less affected by salt tectonics allowing to compare with the strongly deformed Steering Cube I.

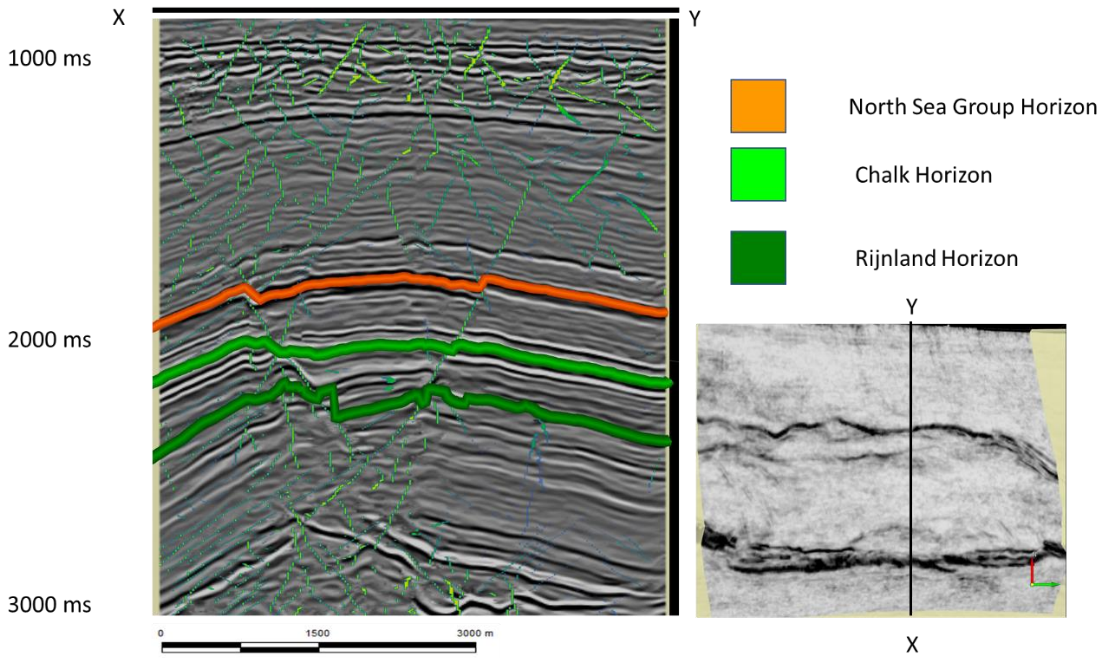

Figure 10.Cross line (X-line) 1218 from the secon steering cube.Showing the Fault Enhancement Filter- similarity, rendered with Thinned Fault likelihood

6
Results

6.1 Attributes to enhance faults and fractures

The methodology proposed by (Jaglan Hardeep, 2016) is used to condition the seismic data providing a better and most suitable framework to handle and apply the seismic attributes. The method to obtain information of dip and generate a volume that steers the attributes, enhances and delivers the best framework for the manual interpretation of faults and fractures allowing to determine length scale and orientation characteristics of this geologic features. The procedure shows faulted and fractured zones that were not able to be recognized previously in the in the original seismic volume. In this section the results are presented along with the most representative geometrical attributes calculated in each targeted horizon. The attributes that allowed the most suitable faults and fractures visualization is presented, these attributes are: Similarity computed with Fault Enhancement Filter and rendered with the Thinned Fault Likelihood attribute. The curvature attributes allowed us to get more insight and locate small scale features and analyzed detailed patterns of the faulted areas. The effective selection of the attributes has allowed to capture faults and fractures that were previously unclear, increasing the confidence to pick up faults manually and reducing uncertainty and the bias as interpretation of the faults take place, hence allowing an improved geologic interpretation faults and fractures in seismic.

6.2 Scruff Horizon

The Scruff horizon is present in the South East part from the seismic volume determined as Steering Cube I, the horizon is only present in the syncline that is formed in the eastern part of the salt wall (figure 9). Table 2 provides the values used to calculate the Background Steering cube and the cut of value used to calculate the FEF this is a value necessary to declare when to use the Dip Steered Diffusion Filter and the Dip Steered Median Filter. Figure 11 allows to visualize the similarity attribute applied with the Fault Enhancement Filter.

OpendTect Attribute	Cut off value	Step Out [IL,XL,Z]
Background Steering Cube		Filter [5,5,5]
Fault Enhancement Filter	0.7	
Thinned Fault Likelihood		[1,1,16]

Table 2.Parameters used to create the Background Steering Cube and attributes in Scruff horizon .

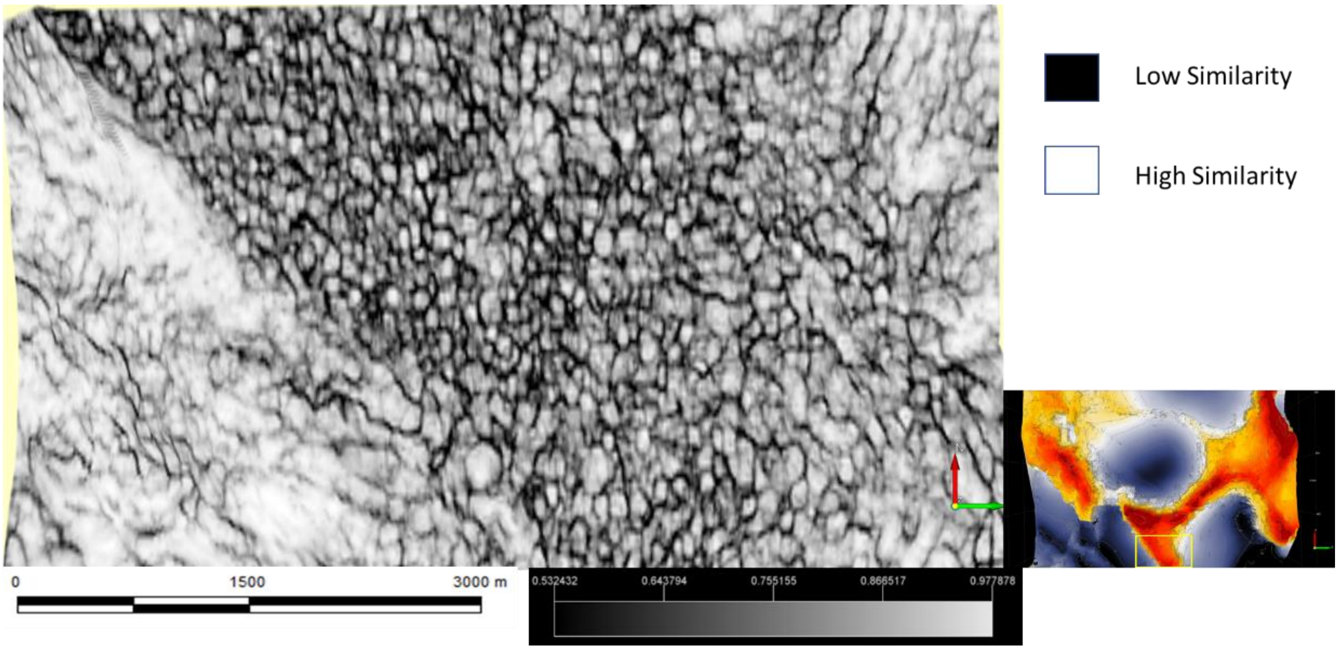

Figure 11.Similarity created with the Fault Enhancement Filter of the Scruff horizon. Bottom right location in the F10 Block.

In the Scruff horizon 58 faults and fractures were characterized table 3 shows the characteristics of the faults evaluated on the Scruff formation.

Scruff formation Steering cube 1	
Number of traced faults and fractures	58
Maximum length (m)	872.45
Minimum length (m)	92.03
Mean (m)	307.95

Table 3.Scruff horizon faults and fractures characterisitcs.

6.2.1 Fault and fracture orientation and length analysis

The fracture length distribution of the interpreted faults and fractures on the Scruff horizon is shown in figure 12. The histogram allows to visualize that the higher frequency of faults and fractures interpreted correspond to lengths ranging from 200 to 400 meters.

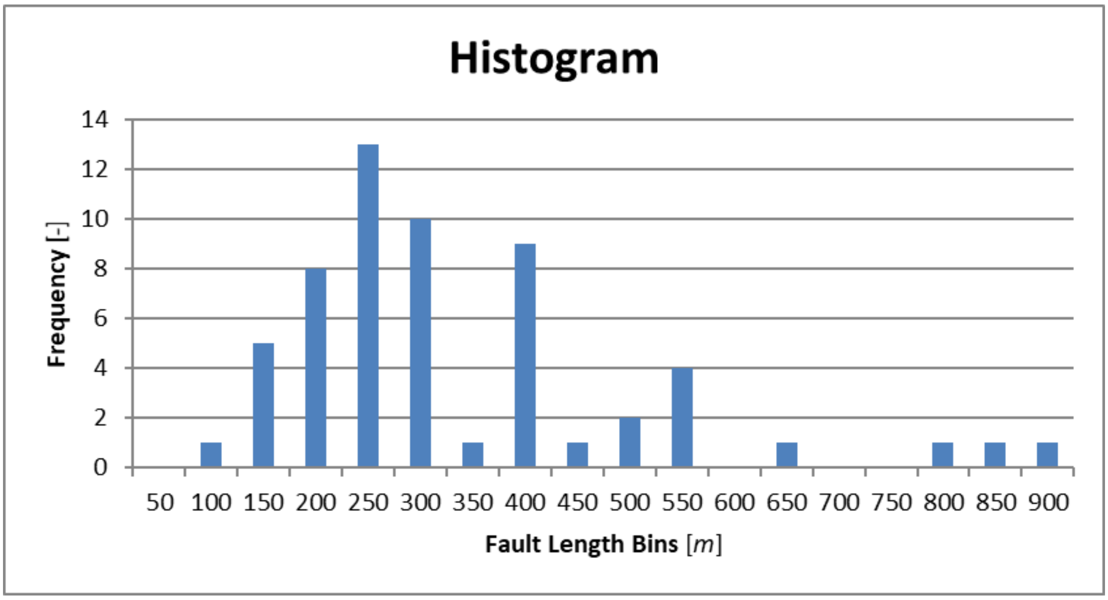

Figure 12.Frequency vs length distribution of the Scruff horizon.

In order to analyze if a relationship between length and orientation exists, the faults and fractures are divided into bin sizes ranging from 0-300 m, 300-600 m and 600-900 m. The histogram in figure 13 shows that the highest number of faults and fractures interpreted enter in the range between 0 and 300 meters the number of faults in this range is 37 and it represents the 63% of the faults and fractures interpreted in the Scruff horizon.

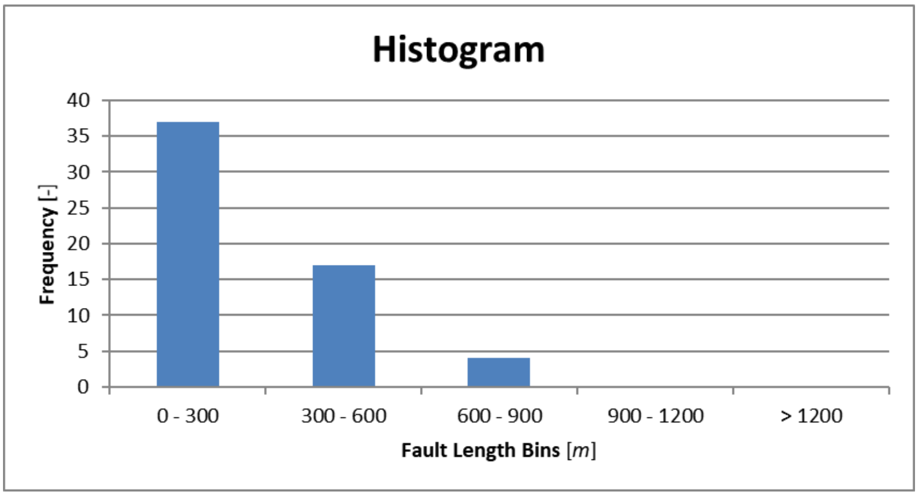

Figure 13.Length distribution vs frequency of the Scruff horizon with different bin size.

The histograms shown in figure 14 allow to visualize the orientation and the frequency for length group. When displaying the orientations for each bin a trend can be observed. The bin size of range 300 m to 600 m shows a preferred orientation and higher frequency between 135º and 150º, as well a more spread orientation for individual faults and fractures.

The trend can also be observed in the histogram for the ranges of 300 to 600 meters, this histogram shows a higher frequency for the faults and fractures
with orientation between 135º and 150º. For the group ranging 600 to 900 meters only three faults entered in this length group and two of them have the orientation ranging 140º and 150º similar to the previous groups. This preferred orientation can also be seen in figure 16, that shows the frequency weighted rose diagram for the Scruff horizon.

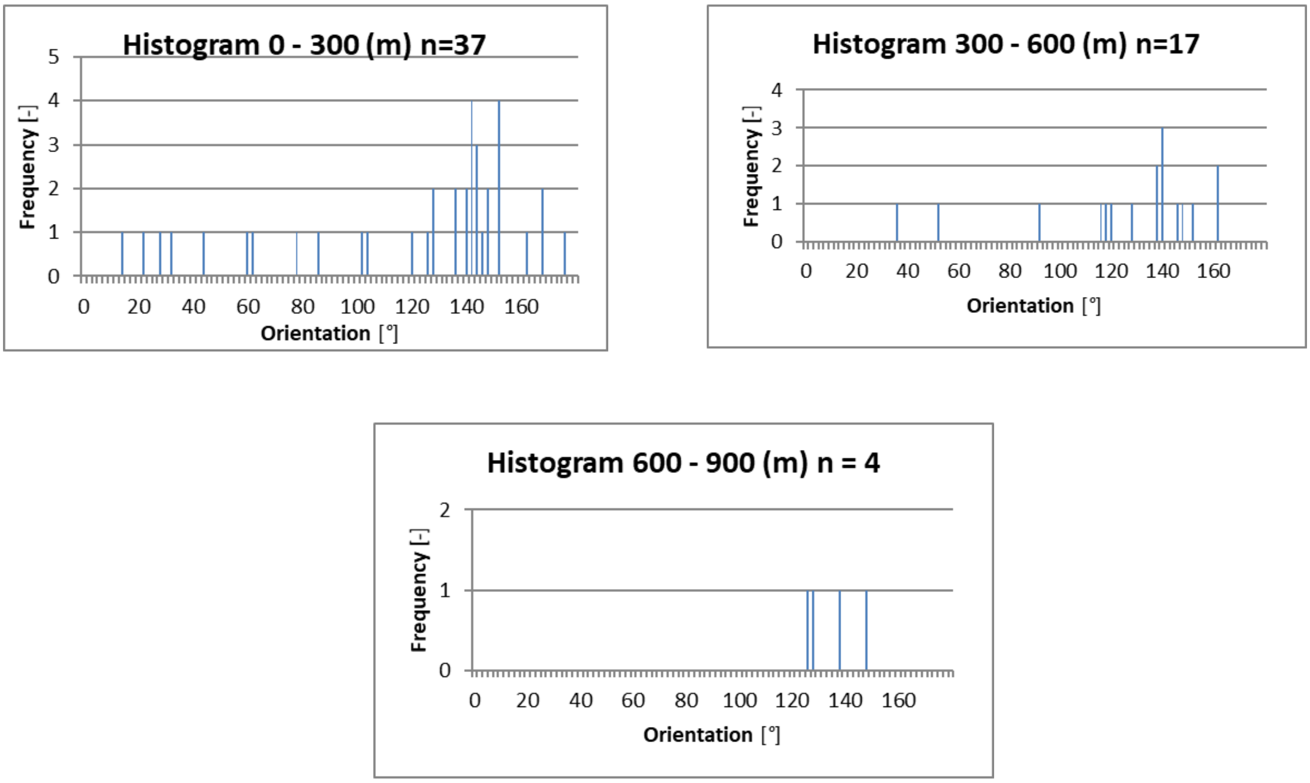

Figure 14.Histograms showing the frequency and orientation of the faults and fractures for different length groups of the Scruff horizon.

Based on this analysis of the rose diagram figure 15 and the orientation histograms (figure 14) a set can be defined and determined for the Scruff formation. The set characteristics are shown in table 4.

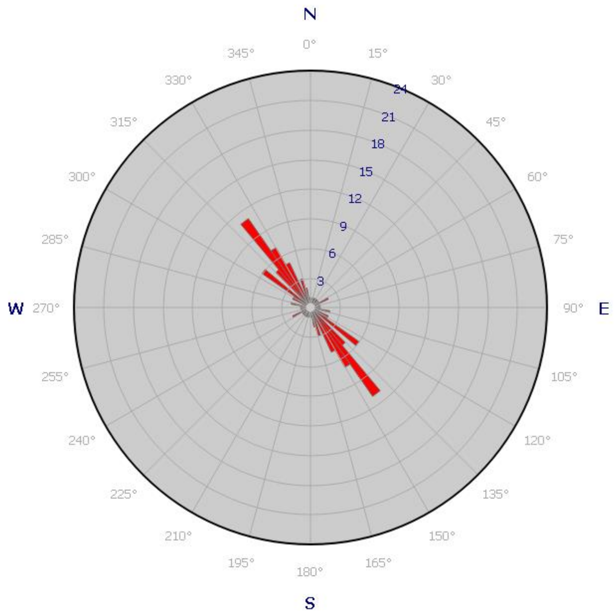

Figure 15.Rose diagram of the Scruff horizon.

Scruff horizon	Set 1
Orientation range	135 º 150 º
Number of faults and fractures	23
Mean length m	323.66

Table 4. Characteristics of the set of faults and fractures of the fault set defined in the interpreted Scruff horizon.

Figure 16 shows the trend line that matches the best to a straight line over the cumulative length distribution of the Scruff formation, the power of law applies for the interval of lengths from 250 m until 1000. For the Scruff horizon the analyzed exponent a value is -2.53 as the slope is negative concluding that the power of law exponent is -2.53 -1 = -3.53.

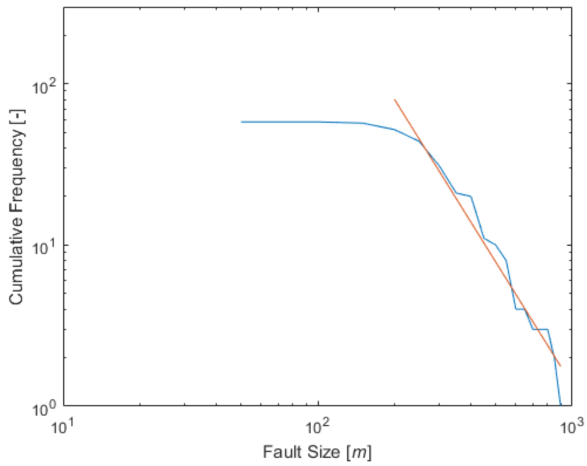

Figure 16. Fracture length vs cumulative frequncy plot of the Scruff Group horizon in log log scale. Evaluation of the power of law.

6.3 Rijnland formation

Results of the evaluation of the seismic attributes are shown in figure 17. The horizon is present on both sides of the salt wall and is present in a vast area of the defined steering cube one in Chapter 3.the horizon is evaluated only in both sides of the synclines formed by the Zechstein wall. Table 5 shows the data used to calculate the Fault Enhancement Filter and the Thinned Fault Likelihood attribute as well the Background Steering Cube used for the calculation.

OpendTect Attribute	Cut off value	Step Out [IL,XL,Z]
Background Steering Cube		Filter [5,5,5]
Fault Enhancement Filter	0.7	
Thinned Fault Likelihood		[1,1,16]

Table 5. Parameters used to create Background Steering Cube and attributes in the Rijnland horizon.

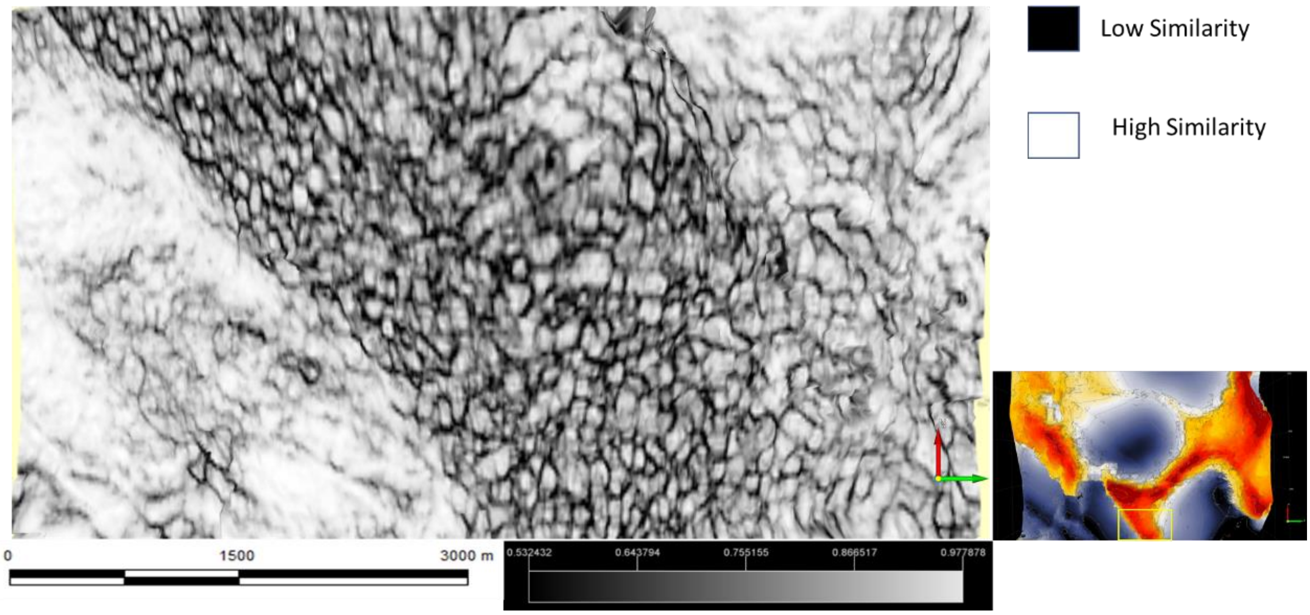

Figure 17. Similarity created with the Fault Enhancement Filter of the Rijnland horizon. Bottom right location in the F10 Block.

Rijnland formation Steering cube 1	
Number of traced faults and fractures	128
Maximum length (m)	1092.19
Minimum length (m)	42.76
Mean (m)	358.39

Table 6. Rijnland horizon faults and fractures characteristics.

6.3.1 Fault and fracture orientation and length analysis

The fracture length distribution of the interpreted faults and fractures on the Rijnland horizon is shown in figure 18. The histogram allows us to visualize that the higher frequency of the faults and fractures interpreted, correspond to lengths ranging from 150 to 350 meters, the largest faults analyzed in the Rijnland horizon is less than 1200 meters.

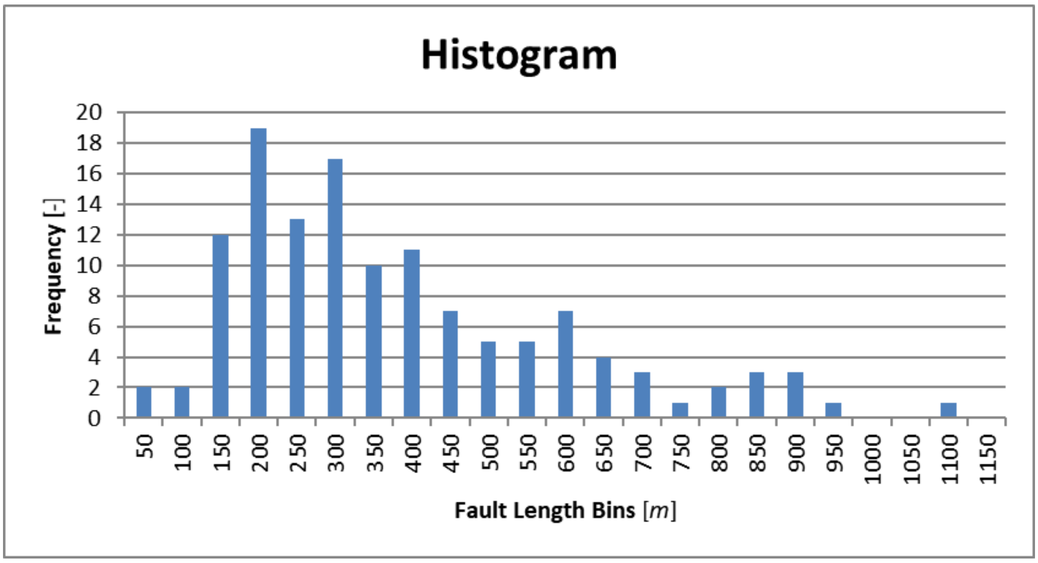

Figure 18.Frequency vs fault length distribution of the Rijnland horizon.

To analyze if a relationship between length and orientation exists, the faults and fractures are divided into bigger bin sizes ranging from 0-300 m, 300-600 m, 600-900 m, and 900-1200 m. The histogram in figure 19 shows that the highest number of faults and fractures interpreted fall in the range between 0 and 300 meters the number of faults in this range is 65 and it represents the 50 % of the faults and fractures interpreted in the Rijnland horizon.

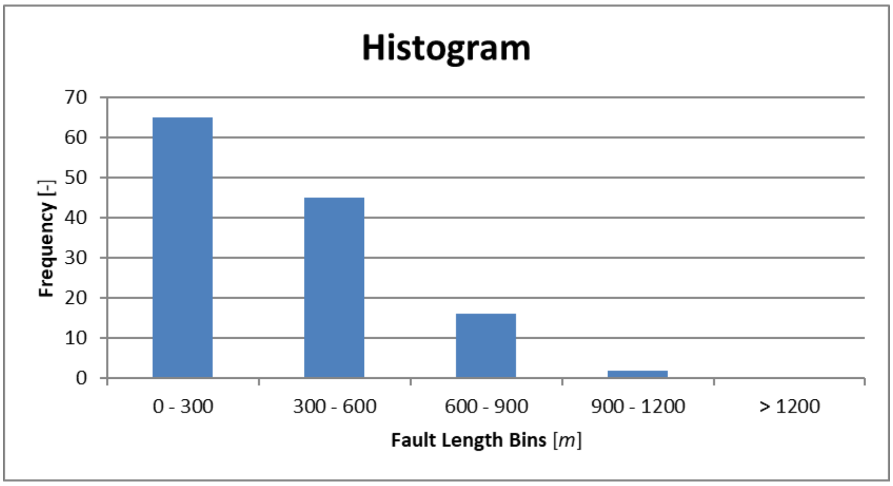

Figure 19.Frequency vs length distribution of the Rijnland horizon.

The histograms shown in figure 20 allow to visualize the orientation for each group. When displaying the orientations for each bin a trend can be observed. The smallest length range of 0 m to 300 m shows a preferred orientation and higher frequency between 120º and 150º, as well a more spread orientation for individual faults and fractures with. The trend can also be observed in the histogram for the ranges of 300 and 600 meters, this histogram shows a higher frequency for the faults and fractures with orientation between 120 and 150º. For the group ranging 600 to 900 meters faults and fractures have the orientation ranging 120º and 140º from reducing the range in comparison to the previous length group. This preferred orientation can also be seen in figure 21 that shows the frequency weighted rose diagram for the Rijnland horizon.

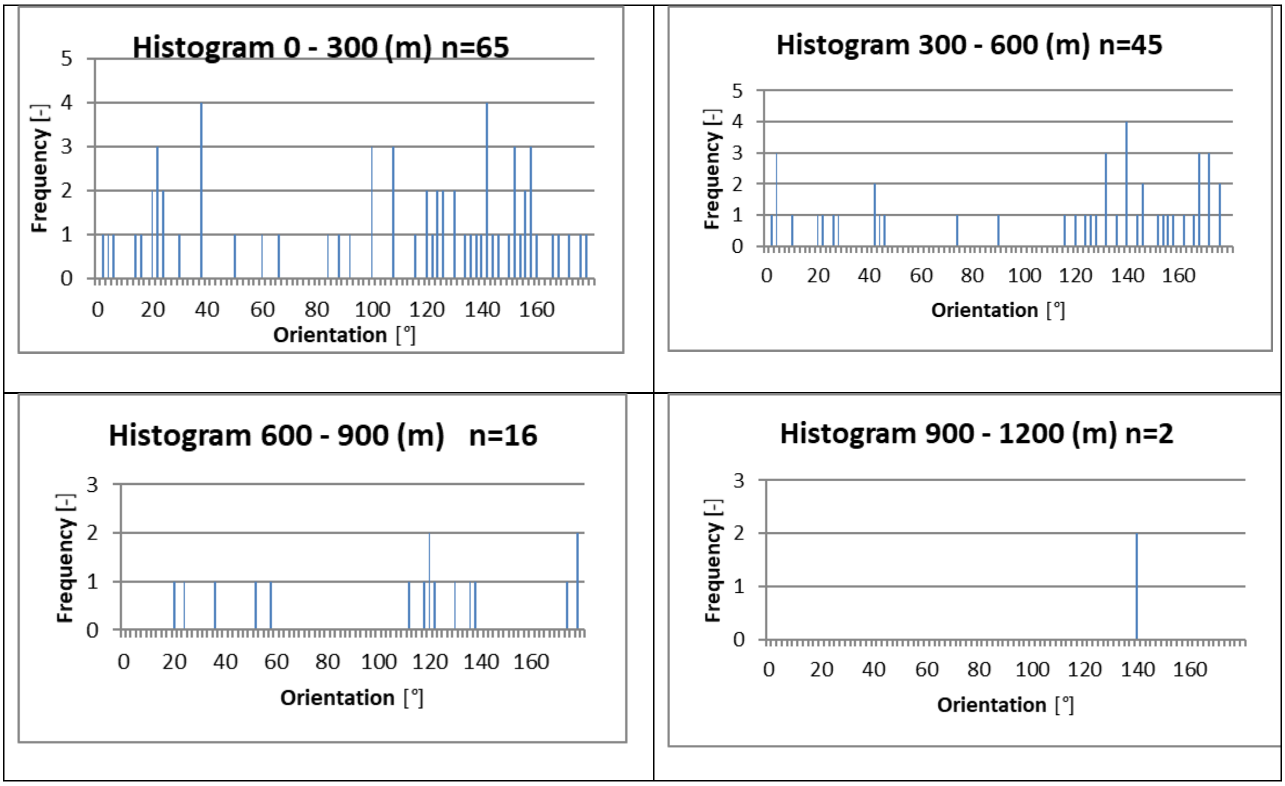

Figure 20.Histograms showing thefrequency and the orientation of faults and fractures for different lenght grups of the Rinjland horizon.

Based on this analysis of the rose diagram in figure 21 and the histograms of figure 20 two sets can be defined and determined for the Rijnland horizon. The set characteristics are shown in table 7 where two sets can be defined and determined.

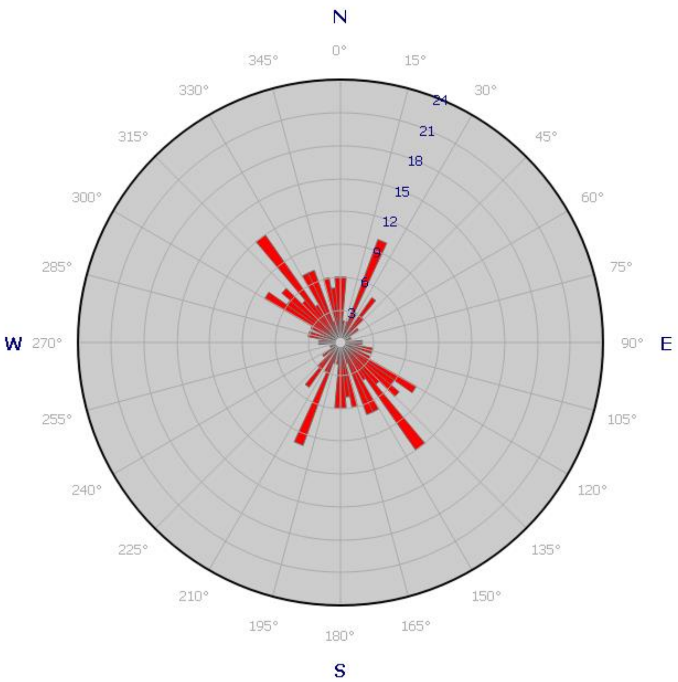

Figure 21.Rose diagram plot of the Rijnland formation.

Rijnland horizon	Set 1	Set 2
Orientation range	120º - 145º	165º -185º
Number of faults and fractures	39	24
Mean length m	133.37	124.61

Table 7.Characteristics of the faults sets of the Rijnland horizon.

Continuing with the analysis of the faults and fractures length, a power of law calculation is done to describe the validated length distribution. Figure 22 shows the cumulative frequency and the length plotted in a log-log scale as well shows the trend line matches to a straight line hence the power of law applies. For the Rijnland horizon the analyzed exponent a value is -2.83 as the slope is negative concluding that the power of law exponent is: -2.83-1=-3.83. This trend line only matches to the lengths between 300 and 1000 meters.

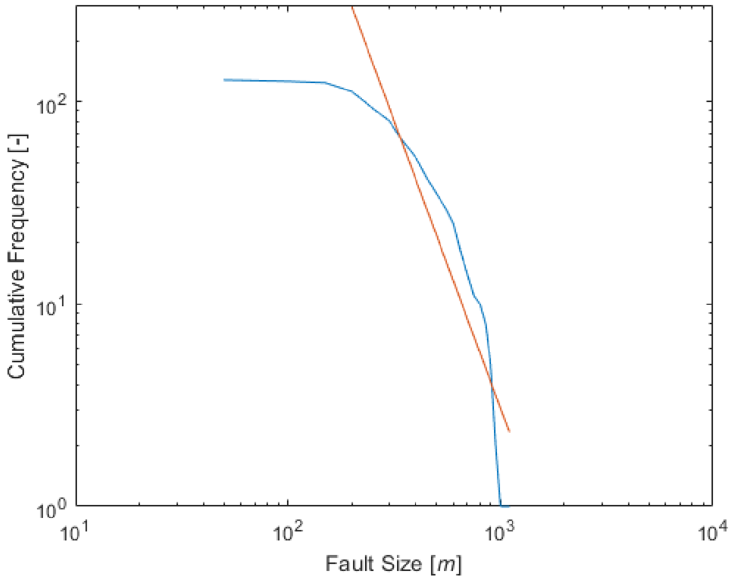

Figure 22. Fracture length vs cumulative frequncy plot of the Rijnland Group horizon in log log scale. Evaluation of the power of law.

6.4 Chalk horizon

The evaluation of the seismic attribute similarity calculated in the Chalk group horizon is illustrated in figure 23.Table 8 shows the values used for the evaluation of the Fault Enhancement Filter, the Background Steering Cube and the Thinned Fault likelihood.

OpendTect Attribute	Cut off value	Step Out [IL,XL,Z]
Background Steering Cube		Filter [5,5,5]
Fault Enhancement Filter	0.6	
Thinned Fault Likelihood		[1,1,16]

Table 8.Parameter used to create the Background Steering Cube and Attribute sin the Chalk Group horizon

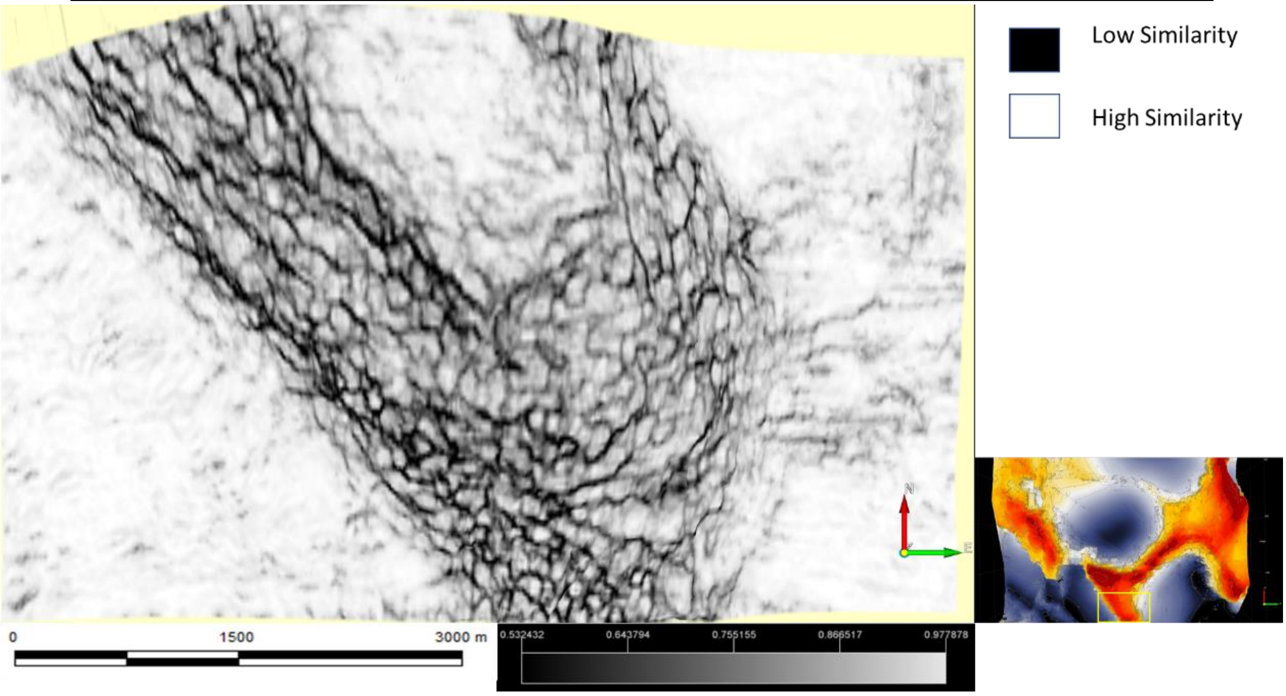

Figure 23. Similarity created with the Fault Enhancement Filter of the Chalk horizon. Bottom right location in the F10 Block.

Chalk formation Steering cube 1	
Number of traced faults and fractures	204
Maximum length (m)	1623.19
Minimum length (m)	42.76
Mean (m)	414.15

Table 9.Chalk Group horizon faults and fractures characteristics

6.4.1 Fault and fracture orientation and length analysis

The fracture length distribution of the interpreted faults and fractures on the Chalk horizon is shown in figure 24. The histogram allows us to visualize that the higher frequency of the faults and fractures interpreted, correspond to lengths ranging from 250 to 450 meters, the largest faults analyzed in the Chalk horizon is less than 1650 meters.

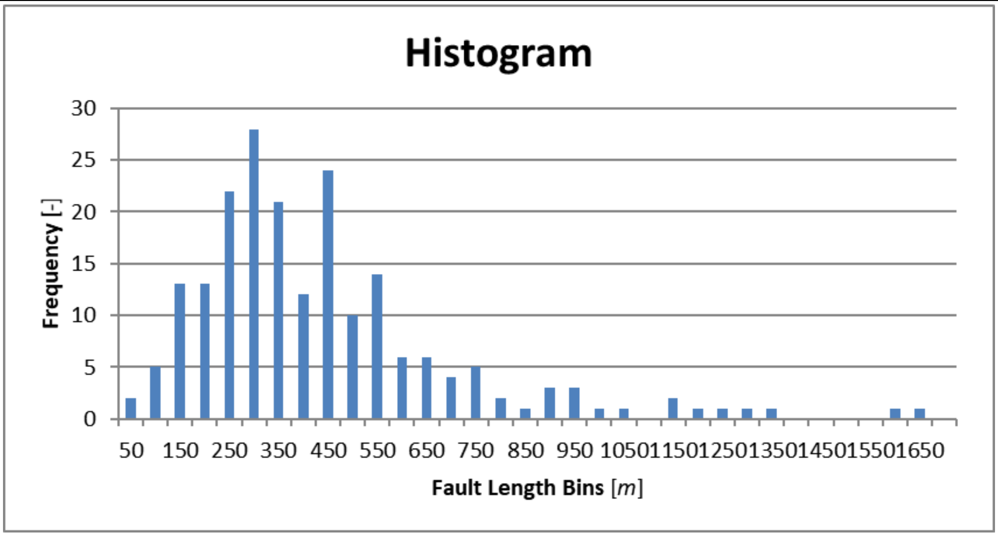

Figure 24.Frequency vs length distribution of the of the Chalk group horizon.

In order to analyze if a relationship between length and orientation exists, the faults and fractures are divided into bigger bin sizes ranging from 0-300 m, 300-600 m, 600-900 m, 900-1200 m and >1200.The histogram in figure 25 shows that the highest number of faults and fractures interpreted fall in the range between 300 and 600 meters the number of faults in this range is 85 and it represents the 41 % of the faults and fractures interpreted in the Chalk horizon.

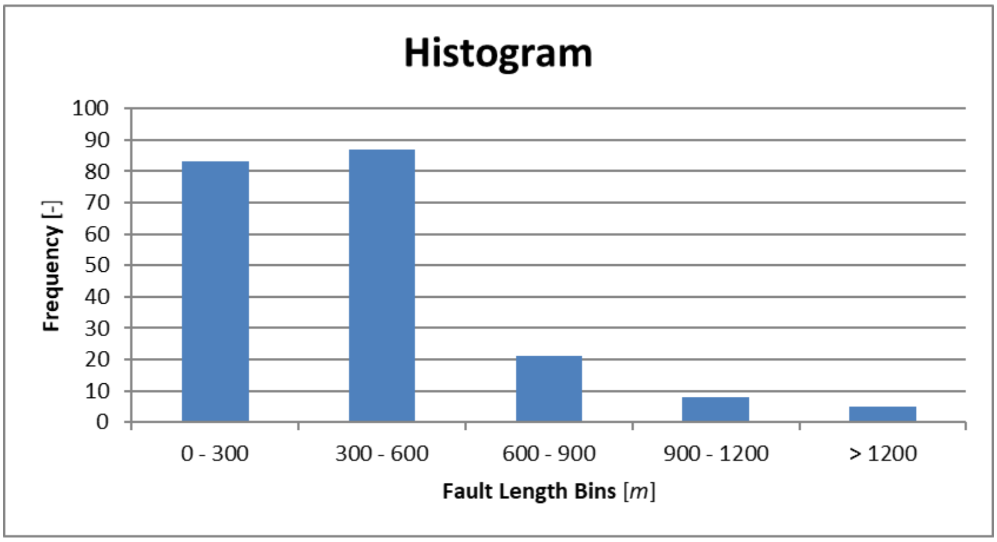

Figure 25.Frequency vs length distribution with different bin size.

The histograms shown in Figure 26 allow to visualize orientations for each group as done for the previous horizons. When displaying the orientations for each group two over all trends can be defined. The smallest bin size shows a higher spread in orientation with some peaks of higher frequency between 120º and 145º also in the range of 160º to 180º. This length range as well shows spread orientation for individual faults and fractures with low frequencies. The trend remains in the histogram for the ranges of 300 m and 600 m where the peaks orientations of 120º to 145º and some peaks in the 0º to 5º and 175 º180º. For the group ranging 600 to 900 the frequency is reduced and the only trend to be characterized is between 125º and 145º. For the range between 900 and 1200 meters fractures enter to the trend observed in previous length groups of 120º and 145º.Finally the larger scale structures above 1200 meters enter this same orientation of 120º to 145º.

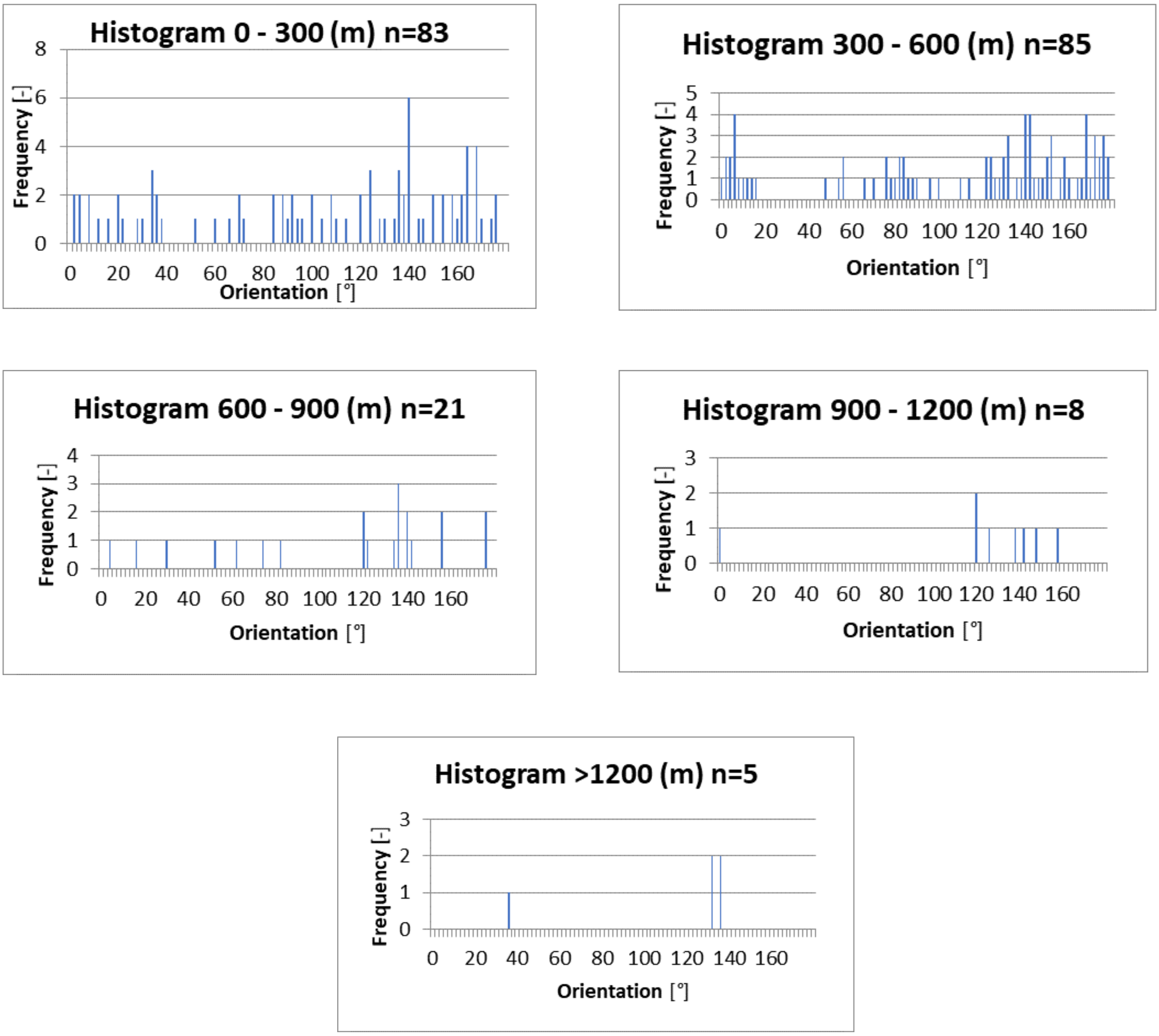

Figure 26. Histograms showing thefrequency and the orientation of faults and fractures for different lenght grupsof the Chalk group horizon.

Based on this analysis of the rose diagram of figure 27 and the histograms of figure 26 two sets can be defined and determined for the Chalk horizon. The set characteristics are shown in table 10.

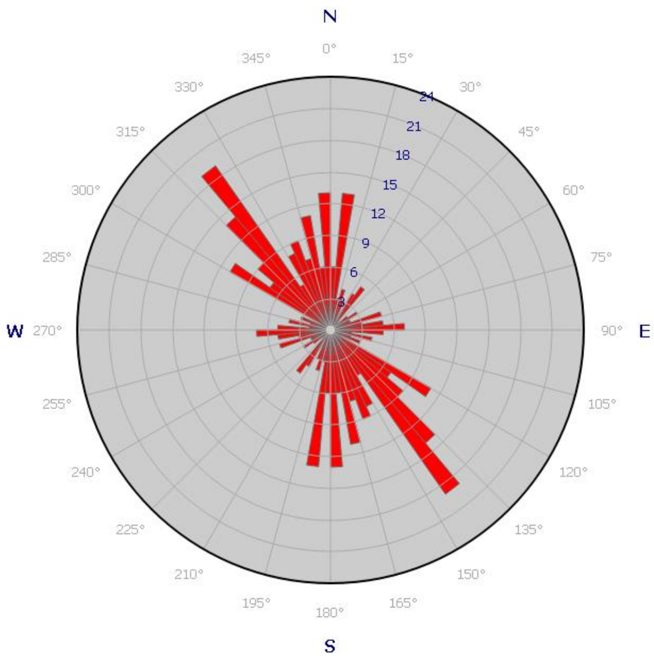

Figure 27.Rose diagram showing the orientation of the faults and fractures interpreted on the Chalk group horizon.

Chalk horizon	Set 1	Set 2
Orientation range	120º - 147º	165º -185º
Number of faults and fractures	57	47
Mean length m	525.11	386.35

Table 10.Characteristics of the fault sets of the Chalk Group horizon.

The power of law calculation is done to describe the validated length distribution. Figure 28 shows the cumulative frequency and the length plotted in a log-log scale as well the trend line matches to a straight line hence the power of law applies. For the Chalk horizon the analyzed exponent a value is -2.34 as the slope is negative concluding that the power of law exponent is: -2.34-1=-3.34. This trend line only matches to the lengths between 200 and 1000 meters.

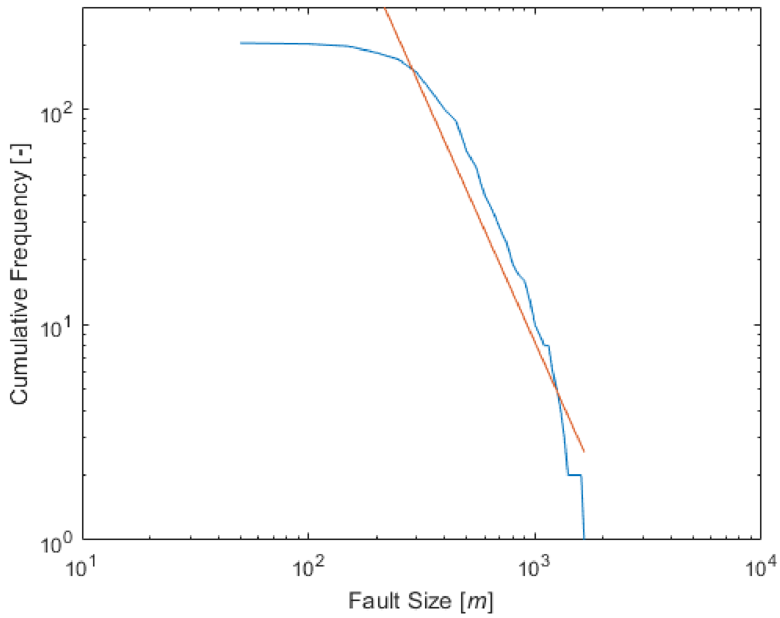

Figure 28. Fracture length vs cumulative frequncy plot of the Chalk Group horizon in log log scale

6.5 North Sea Group

The evaluation of the seismic attribute similarity calculated in the North Sea Group horizon group horizon is illustrated in figure 28. Table 11 shows the values used for the evaluation of the Fault Enhancement Filter, the Background Steering Cube and the Thinned Fault likelihood.

OpendTect Attribute	Cut off value	Step Out [IL,XL,Z]
Background Steering Cube		Filter [5,5,5]
Fault Enhancement Filter	0.7	
Thinned Fault Likelihood		[1,1,16]

Table 11. Parameters usedto create the Bakground Steering cube and attributes of the North Sea Group horizon.

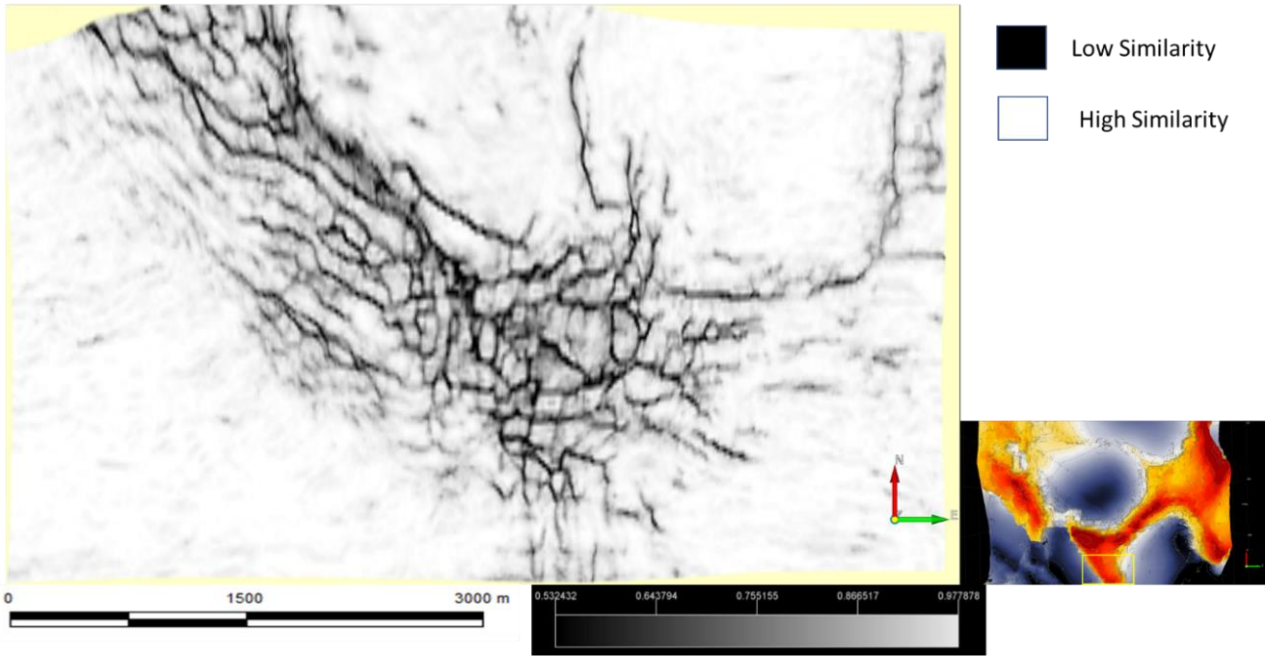

Figure 29. Similarity created with the Fault Enhancement Filter of the North Sea Group horizon. Bottom right location in the F10 Block.

Table 12 shows the characteristics of the number of faults and fractures characterized in the North Sea Group horizon.

Top North Sea Group Steering cube 1	
Number of traced faults and fractures	191
Maximum length (m)	1580.93
Minimum length (m)	39.04
Mean (m)	334.79

Table 12. North Sea Group horizon faults and fractures characteristics.

6.5.1 Fault and fracture orientation and length analysis

The fracture length distribution of the interpreted faults and fractures on the North Sea Group horizon is shown in figure 30. The histogram allows us to visualize that the higher frequency of faults and fractures interpreted correspond to lengths ranging from 150 to 250 meters, the largest faults analyzed in the North Sea Group horizon is less than 1600 meters.

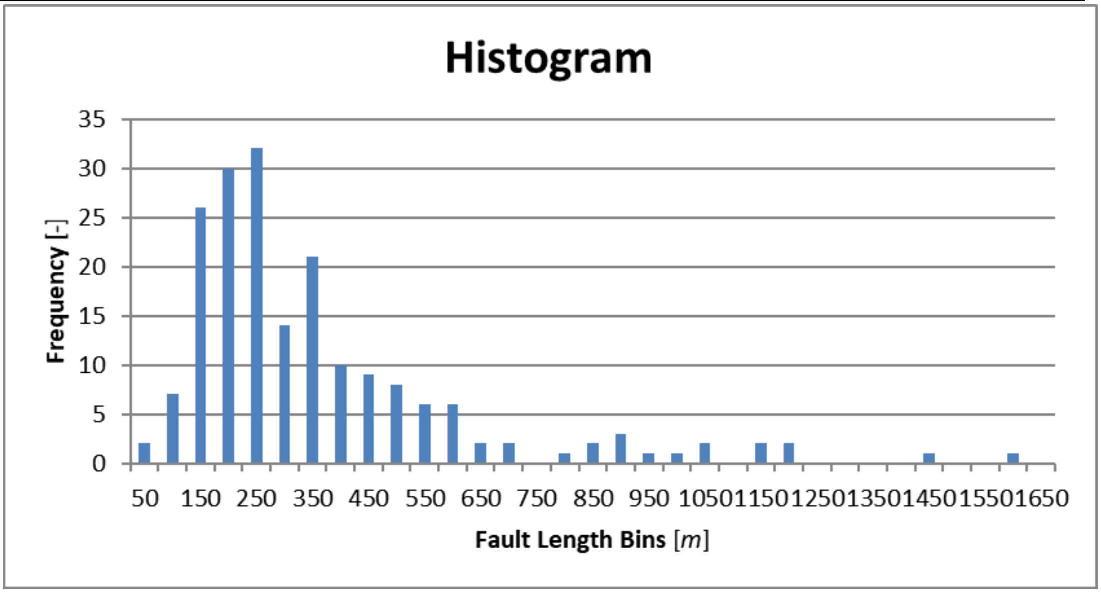

Figure 30. Frequency vs length distribution of the of the North Sea Group group horizon.

In order to analyze if a relationship between length and orientation exists, the faults and fractures are divided into bigger bin sizes ranging from 0-300 m, 300-600 m, 600-900 m, 900-1200 m and >1200.The histogram in figure 31 shows that the highest number of faults and fractures interpreted fall in the range between 0 and 300 meters the number of faults in this range is 111 and it represents the 58 % of the faults and fractures interpreted in the North Sea Group horizon.

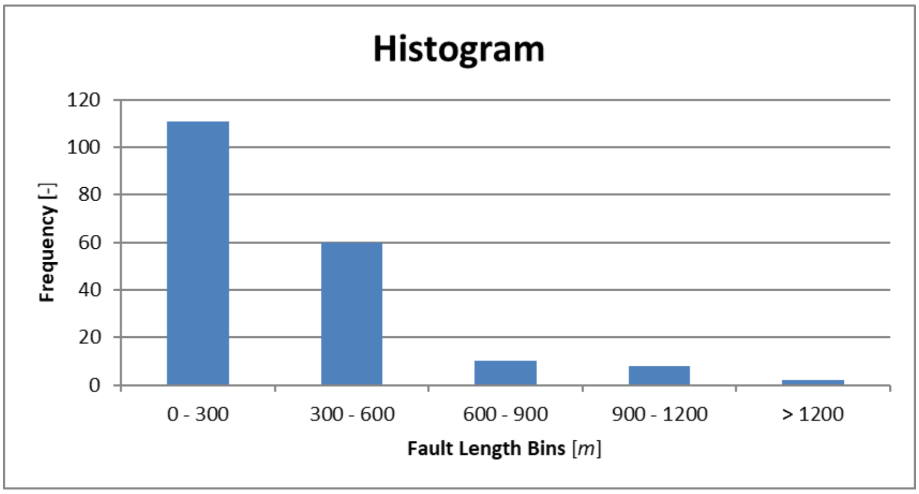

Figure 31. Frequency vs length distribution with different bin size.

The histograms shown figure 32 allow to visualize orientation for each group as done for the previous horizons. When displaying the orientations for each group a trend can be observed. The smallest bin size shows a higher spread in orientation with some peaks of higher frequency between 120º and 150º, also in the range of 160º to 180º. This length range as well shows more spread orientation for individual faults and fractures. The trend remains in the histogram for the ranges of 300 m and 600 m where the peaks orientations of 120º to 150º and some peaks in the 0º to 10º and 160 º180º. For the group ranging 600 to 900 the frequency is reduced and the only trend to be characterized is between 120º and 130º. For the range between 900 and 1200 meters fractures enter to the trend observed in previous length groups of 120º and 145º.Finally the larger scale structure above 1200 meters is oriented orientation 130º.

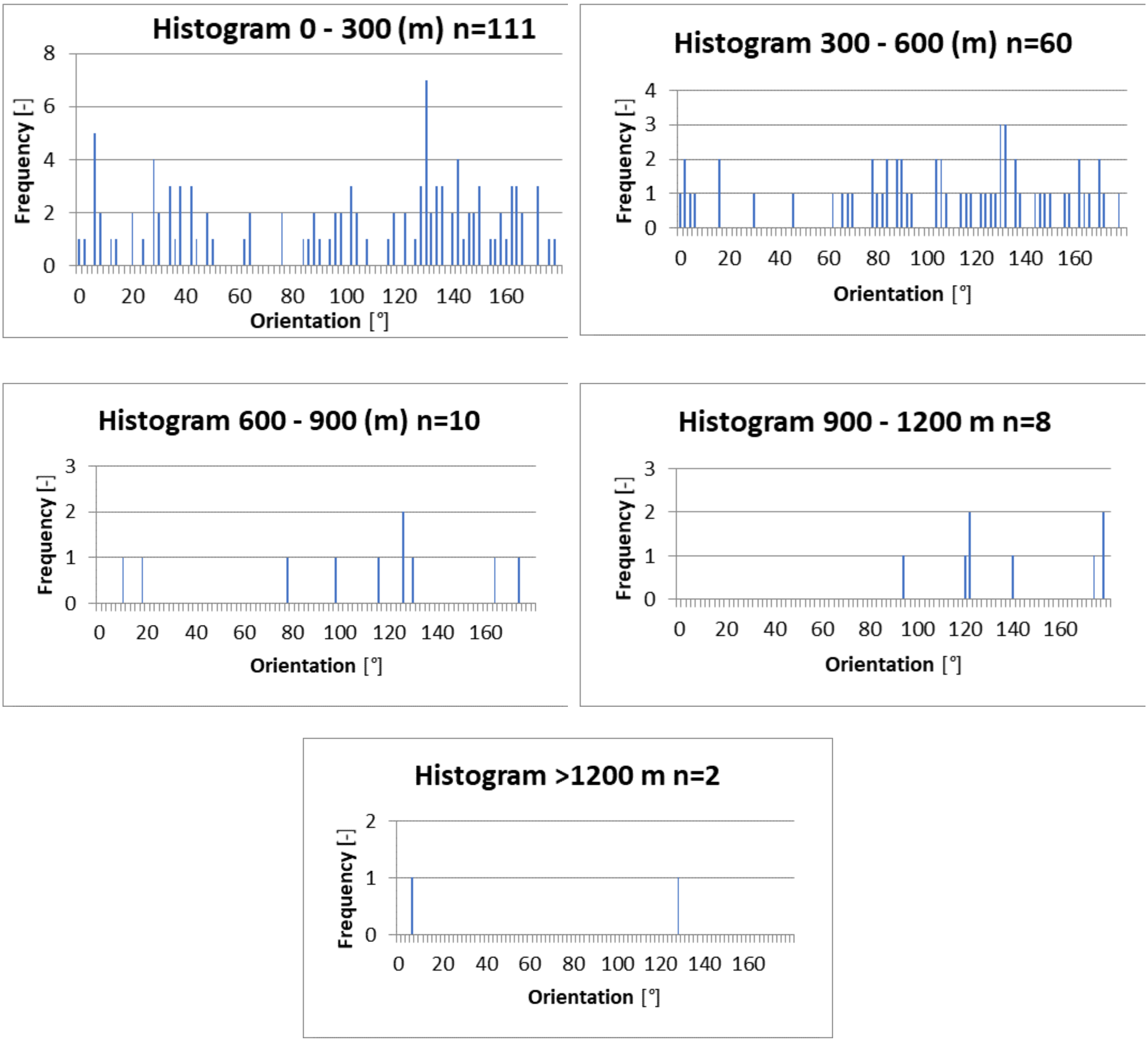

Figure 32. Histograms showing thefrequency and the orientation of faults and fractures for different lenght grupsof the North Sea Group horizon.

Based on this analysis of the rose diagram in figure 33 and the histograms of figure 32 three sets can be defined and determined for the North Sea Group horizon. The set characteristics are shown in table 13.

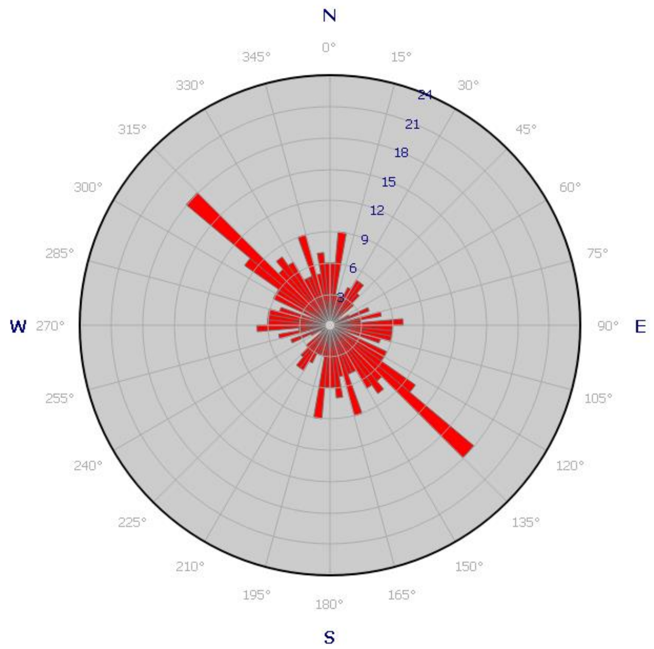

Figure 33. Rose diagram showing the orientation of the faults and fractures interpreted on the North Sea Group horizon.

North Sea Group horizon	Set 1	Set 2	Set 3
Orientation range	120º - 150º	160º -185º	75º – 105º
Number of faults and fractures	58	28	34
Mean length m	357.26	386.36	325.26

Table 13. Characteristics of the fault sets of the North Sea Group horizon.

Continuing with the analysis of the faults and fractures length, a power of law calculation is done to describe the validated length distribution. Figure 34 shows the cumulative frequency and the length plotted in a log-log scale, as well shows the trend line matches a straight line hence the power of law applies. For the North Sea Group horizon, the analyzed exponent a value is -2.34 as the slope is negative concluding that the power of law exponent is: -2.34-1=-3.34. This trend line only matches to the lengths between 200 and 1000 meters.

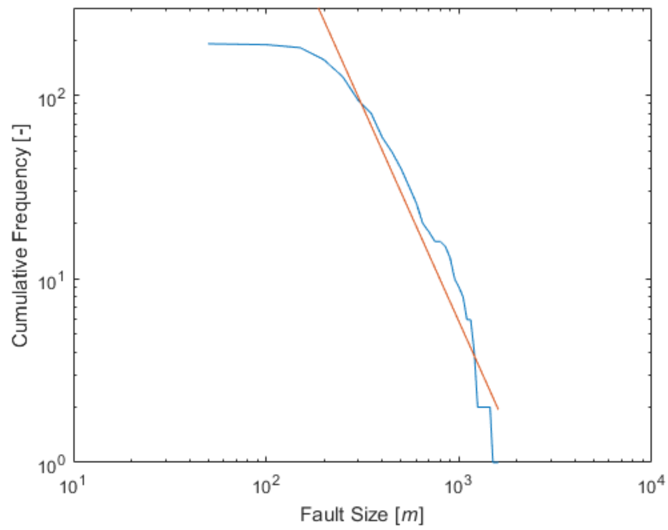

Figure 34. Fracture length vs cumulative frequncy plot of the North Sea Group horizon in log- log scale.

6.6 Second Steering Cube

The second part of this Chapter is devoted to a second Steering Cube located in an area defined and described in Chapter 3. This seismic volume analyzed is located in the most northern part of the seismic survey acquired by Wintershall in the F10 Block. This area was chosen due to the characteristic fault pattern encountered.

6.7 Rijnland horizon

Results of the evaluation of the seismic attributes are shown in figure 35 in the Rijnland horizon. The horizon is present on top of the salt wall and extends to all the area defined as second steering cube in Chapter 3. A salt wall is present with in the area that deformed the horizons of the defined steering cube, Table 14 shows the data used to calculate the Fault Enhancement Filter and the Thinned Fault Likelihood attribute as well the Background Steering Cube used for the calculation.

OpendTect® Attribute	Cut off value	Step Out [IL,XL,Z]
Background Steering Cube		Filter [5,5,5]
Fault Enhancement Filter	0.7	
Thinned Fault Likelihood		[1,1,16]

Table 14. Parameters usedto create the Bakground Steering cube and attributes of the Rijnland Group horizon.

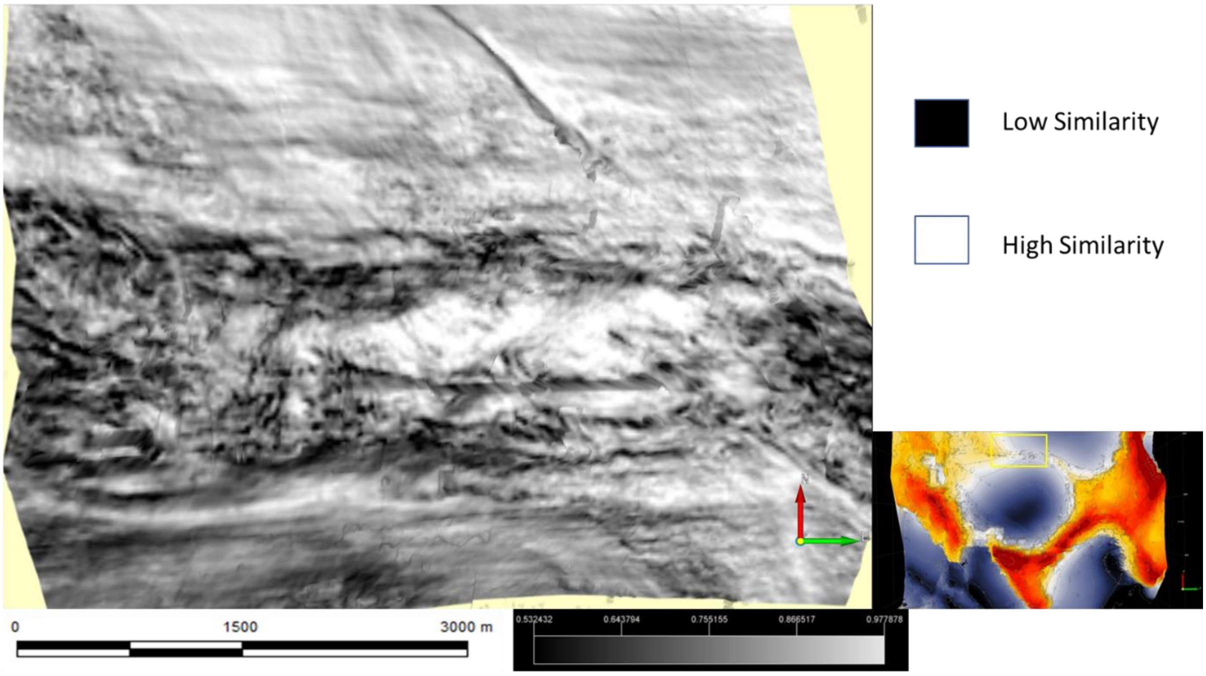

Figure 35. Similarity created with the Fault Enhancement Filter of the Rijnland Group horizon. Bottom right location in the F10 Block.

For the Rijnland horizon a number of 66 faults and fractures were characterized table 15 shows the characteristics evaluated in the Rijnland formation.

Rijnland formation Steering cube 2	
Number of traced faults and fractures	66
Maximum length (m)	2279.96
Minimum length (m)	138.99
Mean (m)	661.57

Table 15. Rijnland Group horizon faults and fractures characteristics.

6.7.1 Fault and fracture orientation and length analysis

The fracture length distribution of the interpreted faults and fractures on the Rijnland horizon is shown in figure 36. The histogram allows us to visualize that the higher frequency of the faults and fractures interpreted, correspond to lengths ranging from 350 to 750 meters, the largest faults analyzed in the Rijnland horizon is less than 2300 meters.

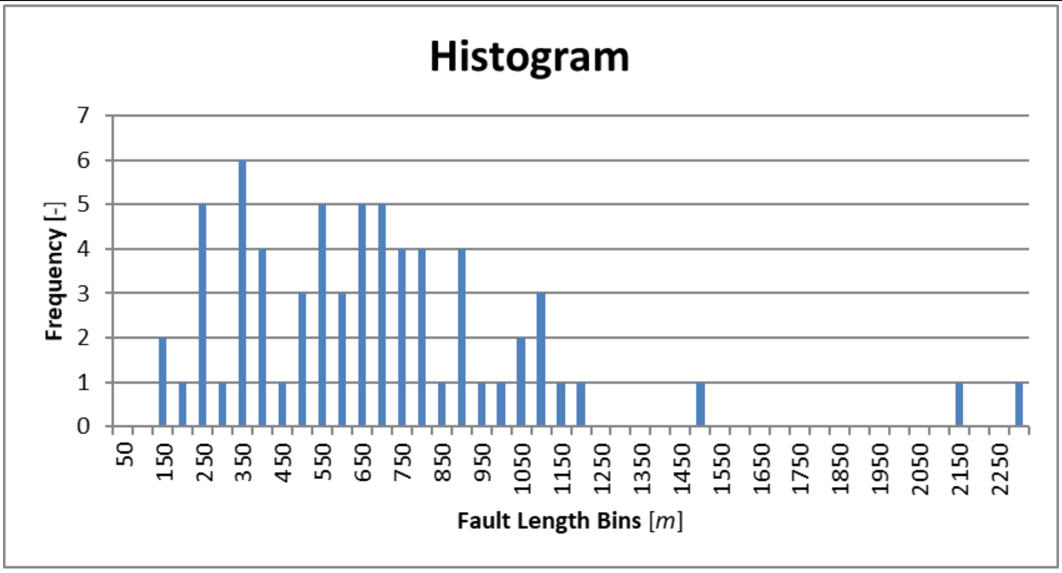

Figure 36. Frequency vs length distribution of the of the Rijnland Group horizon.

In order to analyze if a relationship between length and orientation exists, the faults and fractures are divided into bigger bin sizes ranging from 0-300 m, 300-600 m, 600-900 m, and 900-1200 m and >1200.The histogram in figure 37 shows that the highest number of faults and fractures interpreted fall in the range between 600 and 900 meters the number of faults in this range is 23 and it represents the 34 % of the faults and fractures interpreted in the Rijnland horizon.

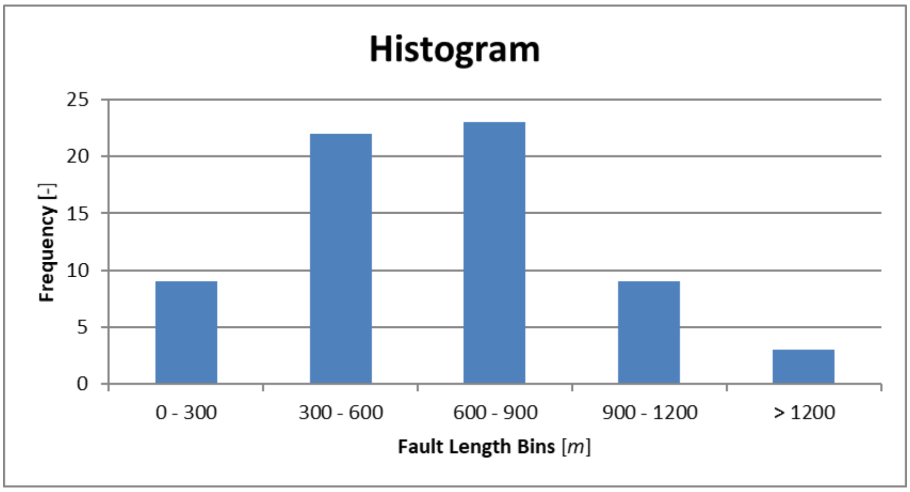

Figure 37. Frequency vs length distribution with different bin size.

The histograms shown in Figure 39 allow to visualize the orientation for each length group. When displaying the orientations for each length range a trend can be observed, except for the smallest range of 0 m to 300 m that mostly is a spread orientation and low frequency values for faults and fractures. Analyzing the length group ranging from 300 m to 600 meters the frequency of faults increases and show spread orientation with a peak in the 90º orientation. This trend can also be observed in the histogram for the ranges of 600 m and 900 meters, where the frequency peak can be seen at 90º. For the group ranging 900 to 1200 meters faults and fractures have the orientation ranging 85º to 95º. Finally, the bin for large scale features above 1200 m shows a low frequency but follows the trend of 90º orientation that can be seen in the previous groups. This preferred orientation can also be seen in figure 40 that shows the frequency weighted

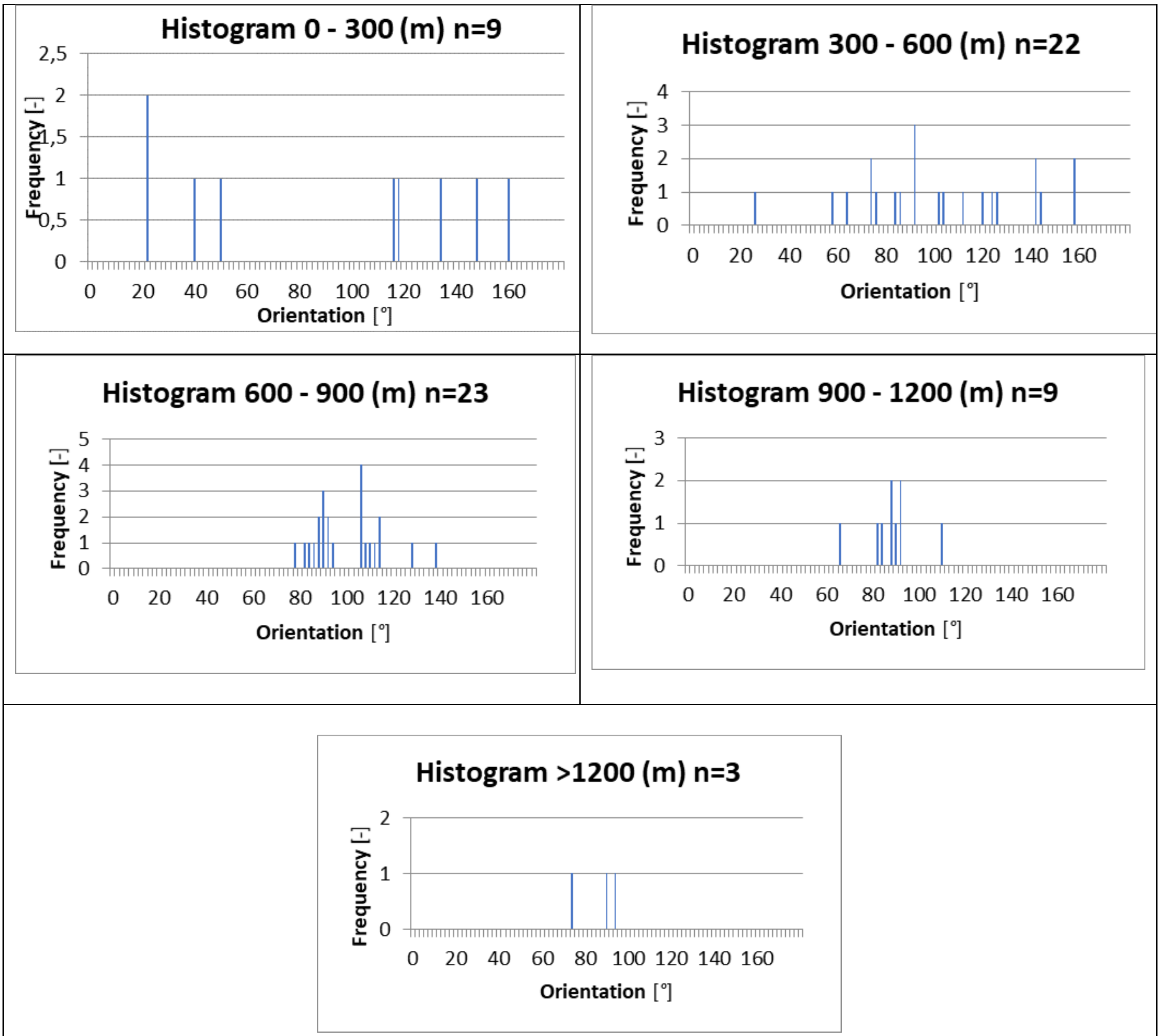

Figure 38Histograms of the

Figure 39. Histograms showing thefrequency and the orientation of faults and fractures for different lenght grupsof the Rijnland Group horizon.

Based on the analysis of the rose diagram of figure 40 and the histograms of figure 39 two sets of can be defined and determined for the Rijnland horizon. The characteristics of the sets can be seen in table 16.

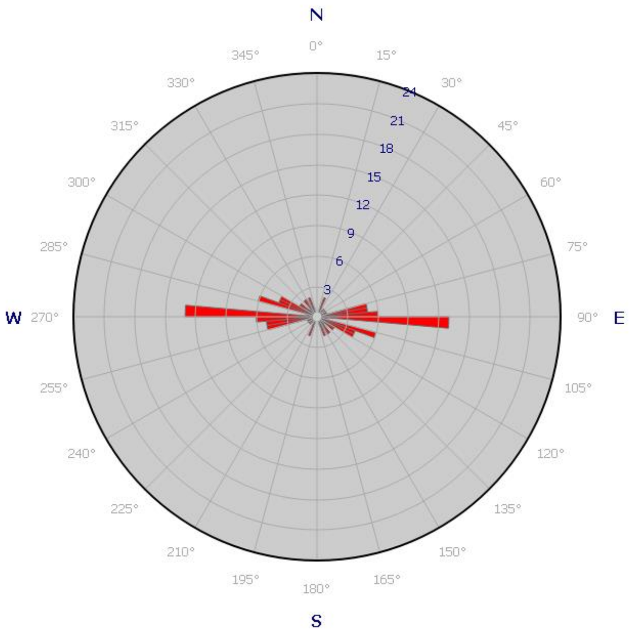

Figure 40. Rose diagram showing the orientation of the faults and fractures interpreted on the North Sea Group horizon.

Rijnland horizon	Set 1	Set 2
Orientation range	75º - 95º	105º - 120º
Number of faults and fractures	30	15
Mean length m	858.26	641.90

Table 16. Characteristics of the fault sets of the Rijnland Group horizon.

Continuing with the analysis of the faults and fractures length, a power of law calculation is done to describe the validated length distribution. Figure 41 shows the cumulative frequency and the length plotted in a log-log scale, also shows the trend line that matches and follows a straight line hence the power of law applies. For the Rijnland horizon the analyzed exponent a value is -1.905 as the slope is negative concluding that the power of law exponent is -1.905 -1 = -2.905. This trend line only matches to the lengths between 200 and 1000 meters.

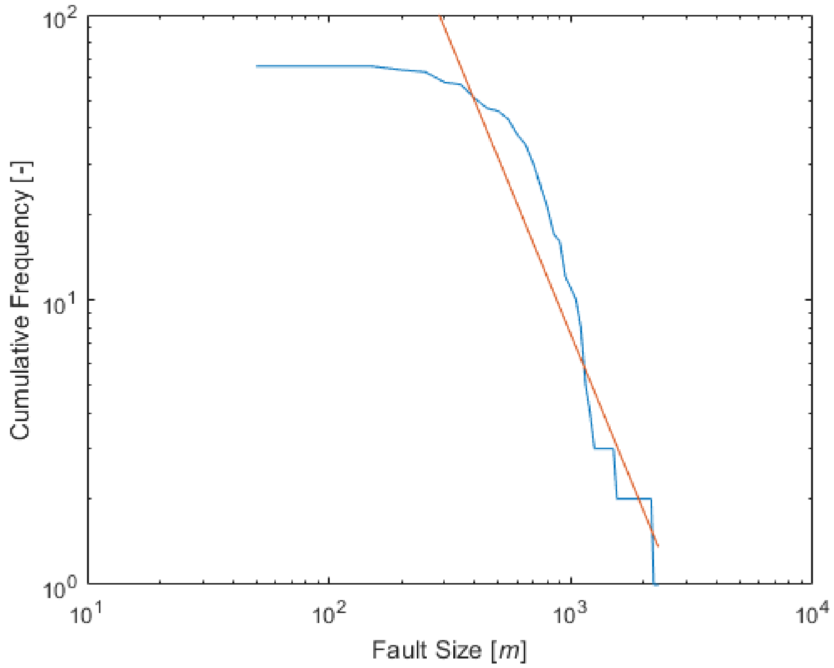

Figure 41. Fracture length vs cumulative frequncy plot of the Rijnland Group horizon in log- log scale.

6.8 Chalk horizon

Results of the evaluation of the seismic attributes are shown in figure 42 in the Chalk horizon. Table 17 shows the data used to calculate the Fault Enhancement Filter and the Thinned Fault Likelihood attribute as well the Background Steering Cube used for the calculation.

OpendTect Attribute	Cut off value	Step Out [IL,XL,Z]
Background Steering Cube		Filter [5,5,5]
Fault Enhancement Filter	0.7	
Thinned Fault Likelihood		[1,1,16]

Table 17. Parameters usedto create the Bakground Steering cube and attributes of the Chalk Group horizon.

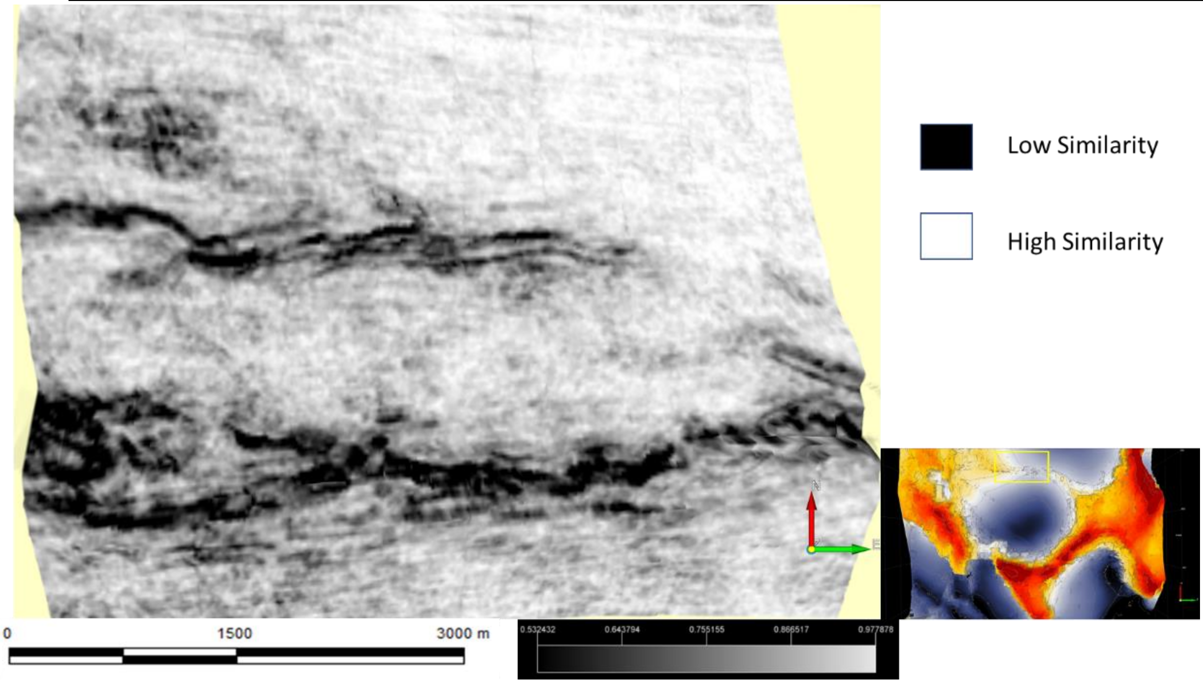

Figure 42. Similarity created with the Fault Enhancement Filter of the Chalk Group horizon. Bottom right location in the F10 Block.

For the Chalk horizon a number of 62 faults and fractures were characterized table 18 shows the characteristics obtained in the Chalk formation.

Chalk formation Steering cube 2	
Number of traced faults and fractures	62
Maximum length (m)	1662.13
Minimum length (m)	63.92
Mean (m)	454.80

Table 18. Chalk Group horizon faults and fractures characteristics.

6.8.1 Fault and fracture orientation and length analysis

The fracture length distribution of the interpreted faults and fractures on the Chalk horizon is shown in figure 43. The histogram allows us to visualize that the higher frequency of the faults and fractures interpreted, correspond to lengths ranging from 200 to 350 meters, the largest faults analyzed in the Chalk horizon is less than 1700 meters.

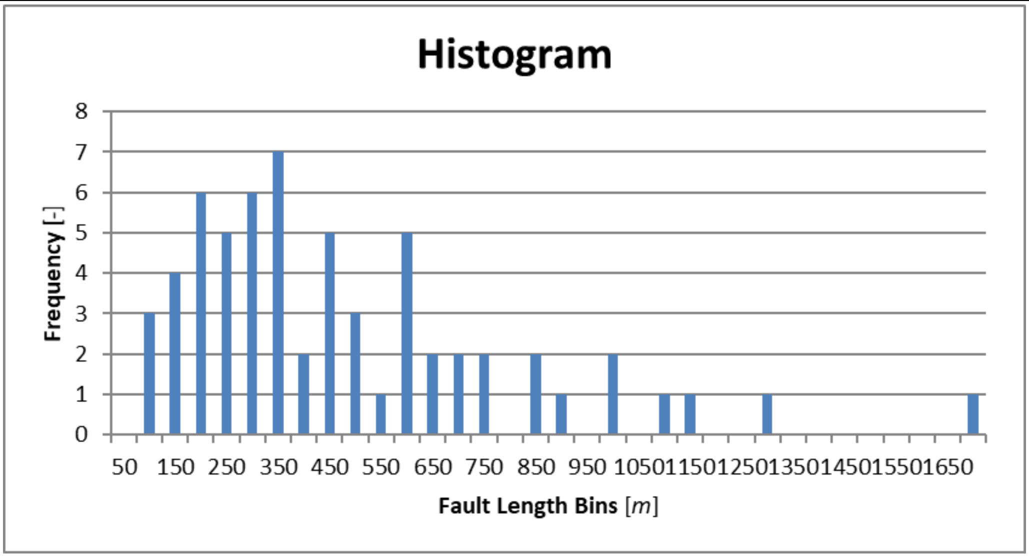

Figure 43. Frequency vs length distribution of the of the Chalk Group horizon.

In order to analyze if a relationship between length and orientation exists, the faults and fractures are divided into bigger bin sizes ranging from 0-300 m, 300-600 m, 600-900 m, and 900-1200 m and >1200.The histogram in figure 44 shows that the highest number of faults and fractures interpreted fall in the range between 0 and 300 meters the number of faults in this range is 24 and it represents the 38 % of the faults and fractures interpreted in the Chalk horizon.

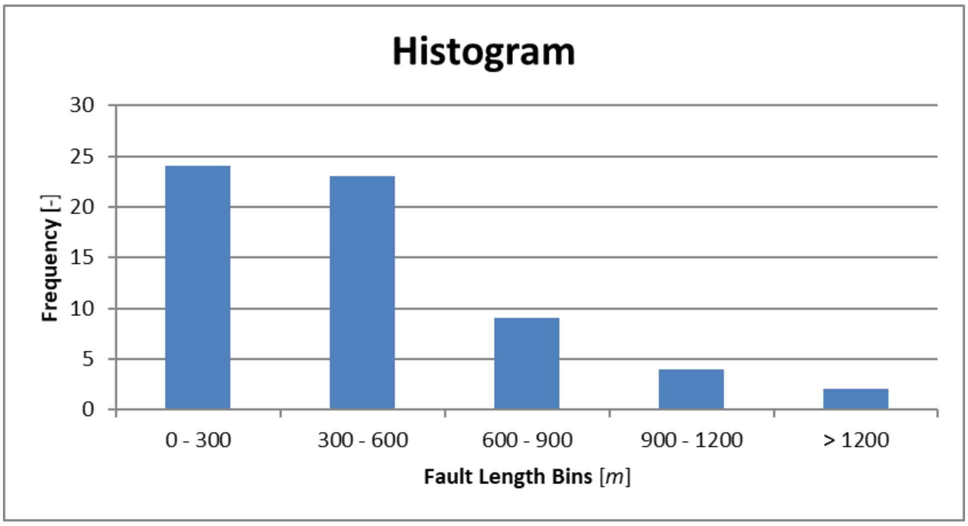

Figure 44. Frequency vs length distribution with different bin size.

The histograms shown in figure 45 allow to visualize the orientation for each group. When displaying the orientations for each length range a trend can be observed, in the length ranging from 0 m to 300 m a preferred orientation in the ranges of 80º to 90º and low frequency values with spread orientation. Analyzing the length group ranging from 300 m to 600 meters the frequency of faults increases and show spread orientation with a peak in the 90º orientation. This trend can also be observed in the histogram for the ranges of 600 m and 900 meters, where the frequency peak can be seen at 90º and also at 110º. For the group ranging 900 to 1200 meters faults and fractures have the orientation ranging 85º to 95º. for large scale features above 1200 m shows a low frequency but follows the trend of 90º orientation that can be seen in the previous groups. This preferred orientation can also be seen in figure 46 that shows the frequency weighted rose diagram for the Chalk horizon.

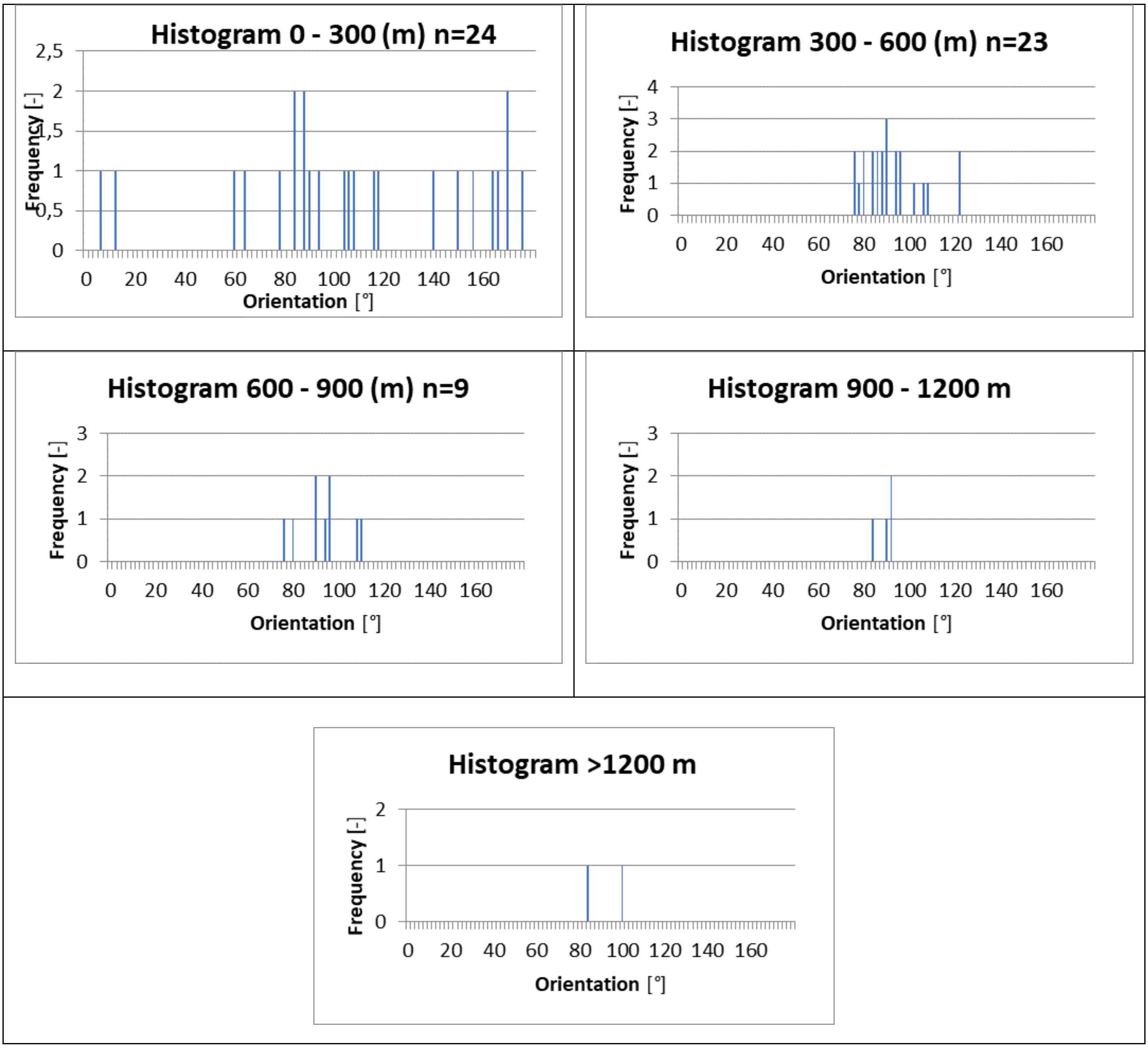

Figure 45. Histograms showing thefrequency and the orientation of faults and fractures for different lenght grupsof the Chalk Group horizon.

Based on the analysis of the Rose diagram of figure 46 and the histograms of figure 45 1 set can be determined for the Chalk horizon. The characteristics of the sets defined are shown in table 19.

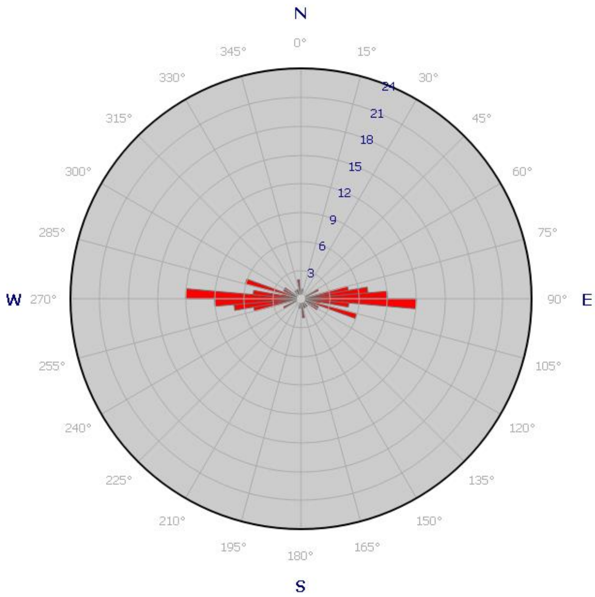

Figure 46. Rose diagram showing the orientation of the faults and fractures interpreted on the Chalk Group horizon.

Chalk horizon	Set 1
Orientation range	75º - 95º
Number of faults and fractures	33
Mean length m	541.26

Table 19. Characteristics of the fault sets of the Chalk Group horizon.

Continuing with the analysis of the faults and fractures length, a power of law calculation is done to describe the validated length distribution. Figure 47 shows the cumulative frequency and the length plotted in a log-log scale, as well shows the trend line that matches and follows a straight line hence the power of law applies. For the Chalk Group horizon slope value -2.26 as the slope is negative concluding that the power of law exponent is: -2.26-1=-3.26. This trend line only matches to the lengths between 250 and 1000 meters.

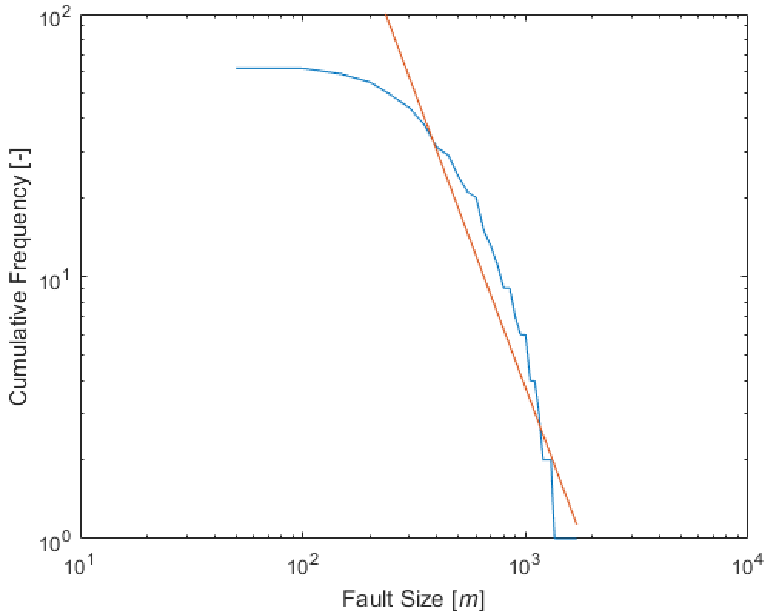

Figure 47. Fracture length vs cumulative frequncy plot of the Chalk Group horizon in log- log scale.

6.9 North Sea Group

Results of the evaluation of the seismic attributes are shown in figure 48 of the North Sea Group horizon. Table 20 shows the data used to calculate the Fault Enhancement Filter and the Thinned Fault Likelihood attribute as well the Background Steering Cube used for the calculation.

OpendTect Attribute	Cut off value	Step Out [IL,XL,Z]
Background Steering Cube		Filter [5,5,5]
Fault Enhancement Filter	0.7	
Thinned Fault Likelihood		[1,1,16]

Table 20. Parameters usedto create the Bakground Steering cube and attributes of the North Sea Group Group horizon.

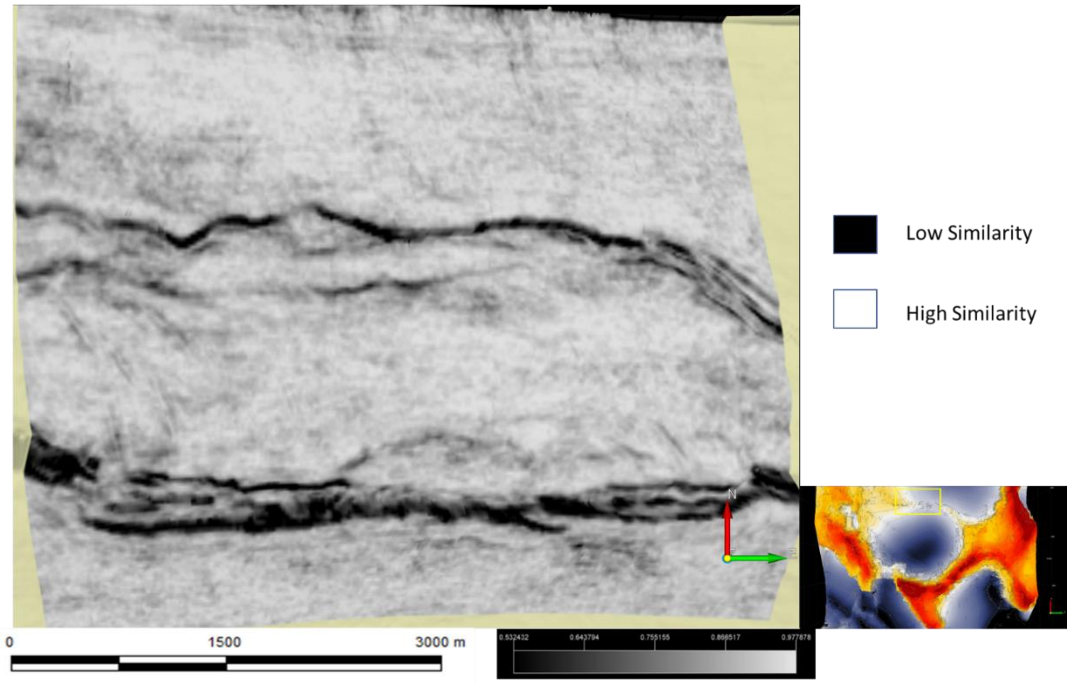

Figure 48. Similarity created with the Fault Enhancement Filter of the North Sea Group horizon. Bottom right location in the F10 Block.

Table 21 shows the characteristics of the faults evaluated in the North Sea Group horizon.

North Sea Group Horizon Steering cube 2	
Number of traced faults and fractures	37
Maximum length (m)	2878.51
Minimum length (m)	163.79
Mean (m)	883.45

Table 21. Chalk Group horizon faults and fractures characteristics.

6.9.1 Fault and fracture orientation analysis

The fracture length distribution of the interpreted faults and fractures on the North Sea Group horizon is shown in figure 49 The histogram allows us to visualize that the higher frequency is 3 and this frequency is found in different lengths of the faults and fractures interpreted, correspond to lengths ranging from 200 to 350 meters, the largest faults analyzed in the North Sea Group horizon is less than 2878.5 meters.

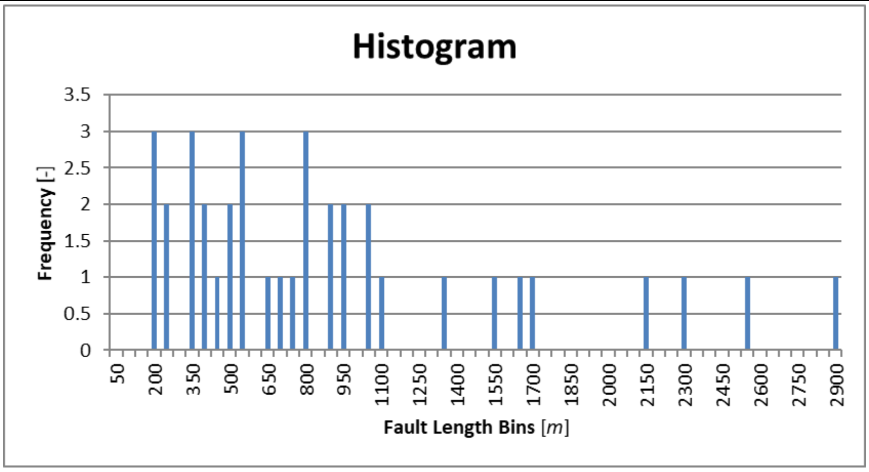

Figure 49. Frequency vs length distribution of the of the North Sea Group horizon.

In order to analyze if a relationship between length and orientation exists, the faults and fractures are divided into bigger bin sizes ranging from 0-300 m, 300-600 m, 600-900 m, and 900-1200 m and >1200.The histogram in figure 50 shows that the highest number of faults and fractures interpreted fall in the range between 300 and 600 meters the number of faults in this range is 11 and it represents the 29 % of the faults and fractures interpreted in the Chalk horizon.

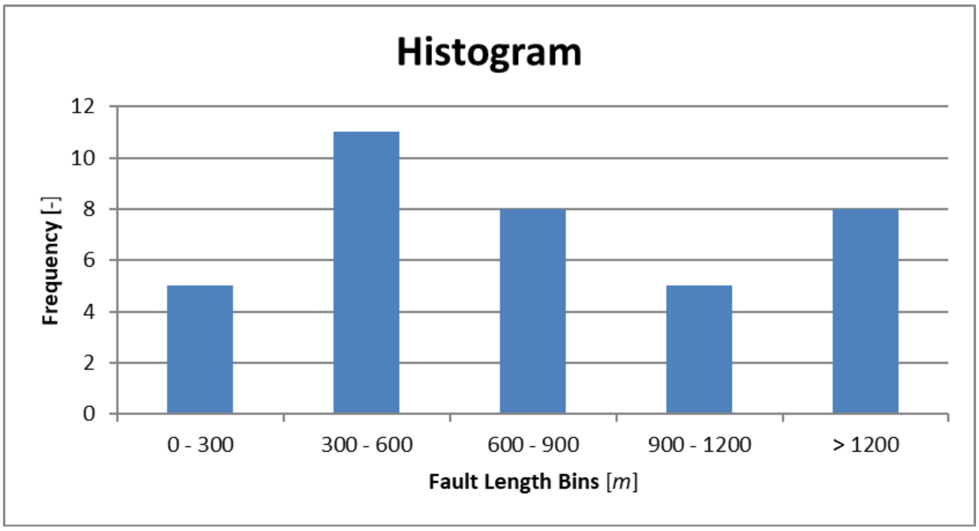

Figure 50. Frequency vs length distribution with different bin size.

The histograms shown in Figure 51 allow to visualize the orientation for each group. When displaying the orientations for each bin a trend can be observed, the bin size ranging from 0 m to 300 m shows preferred orientation and low frequency values for faults and fractures in the range of 97º and 120º. Analyzing the length group ranging from 300 m to 600 meters the frequency of faults is maintained low and show no preferred but they concentrate l in a range between 80º and 120º. This trend can also be observed in the histogram for the ranges of 600 m and 900 meters, where the frequency peak can be seen at 80º enclosing the range until 100. For the group ranging 900 to 1200 meters faults and fractures have the orientation ranging 80º to 100º. Finally, the bin for large scale features above 1200 m shows a low frequency but follows the trend of of previous groups between 80º and 100º orientation. This preferred orientation can also be seen in figure 52 that shows the frequency weighted rose diagram for the North Sea Group horizon.

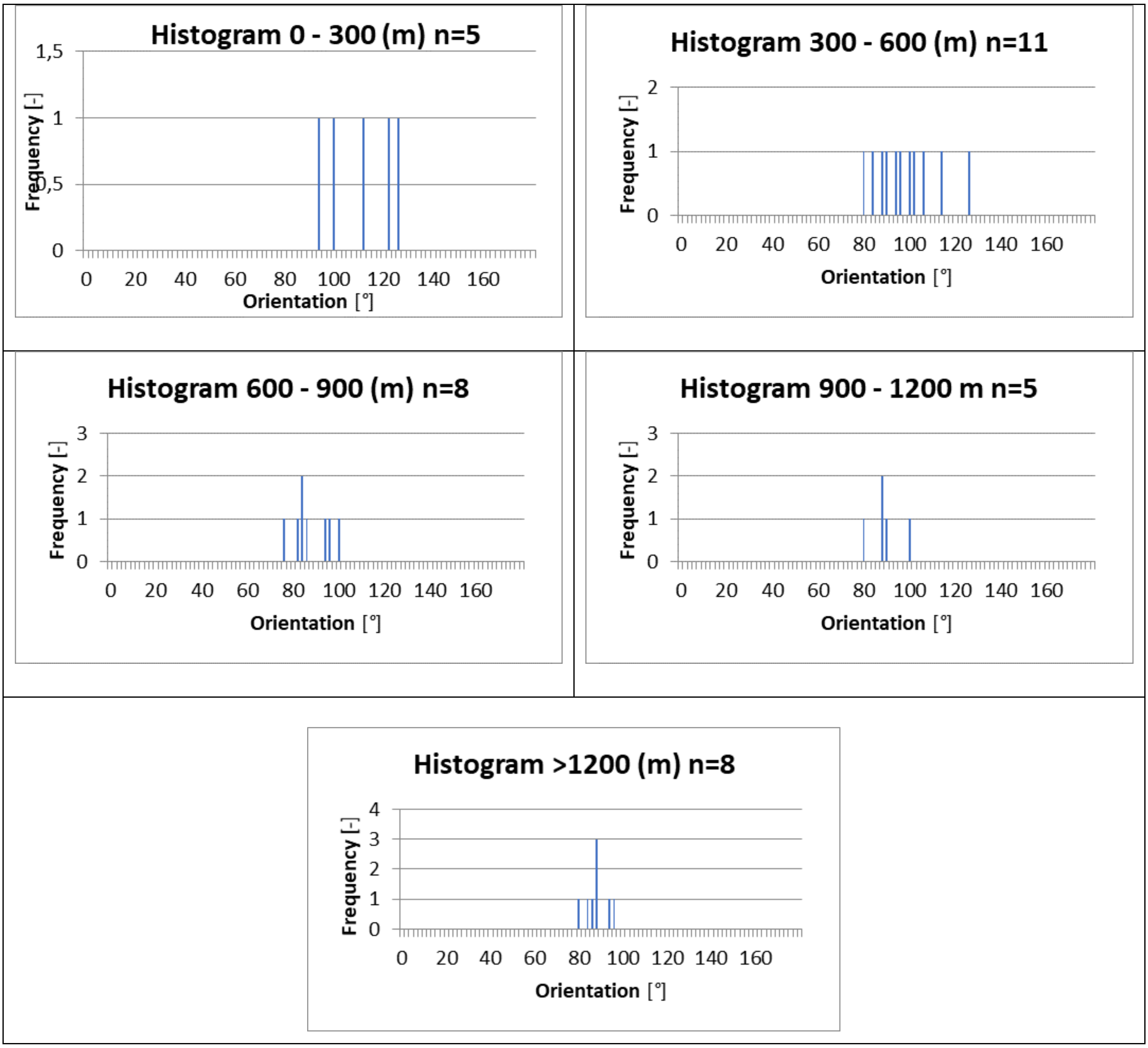

Figure 51. Histograms showing thefrequency and the orientation of faults and fractures for different lenght grupsof the Chalk Group horizon.

Based on the analysis of the rose diagram of figure 52 and the histograms of figure 51 one set can be determined for the North Sea Group horizon. The characteristics of the sets defined are shown in table 22.

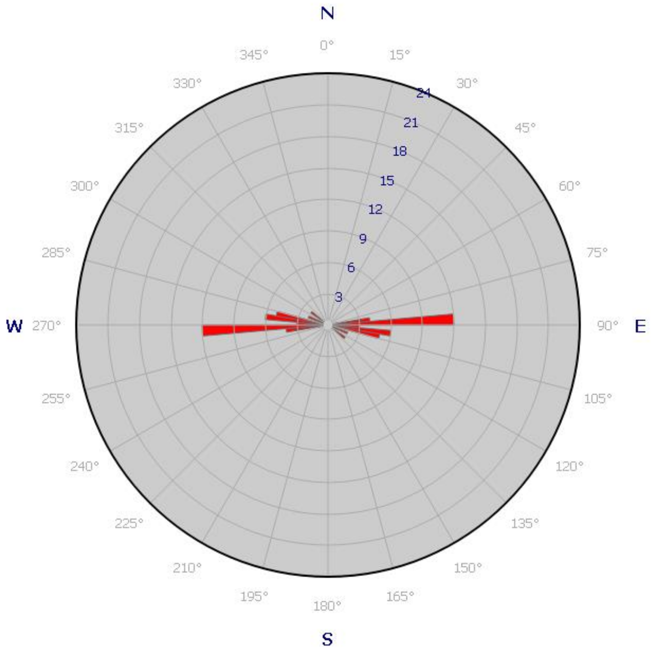

Figure 52. Rose diagram showing the orientation of the faults and fractures interpreted on the North Sea Group horizon.

North Sea Group horizon	Set 1
Orientation range	78.5º - 105º
Number of faults and fractures	31
Mean length m	996.45

Table 22. Characteristics of the fault sets of the North Sea Group horizon.

Continuing with the analysis of the faults and fractures length, a power of law calculation is done to describe the validated length distribution. Figure 53 shows the cumulative frequency and the length plotted in a log-log scale as well shows the trend line that matches to and follows a straight line, hence the power of law applies. For the North Sea Group horizon, the analyzed exponent a value is -1.55 as the slope is negative concluding that the power of law exponent is: -1.55-1=-2.55. This trend line only matches to the lengths between 400 and 1200 meters.

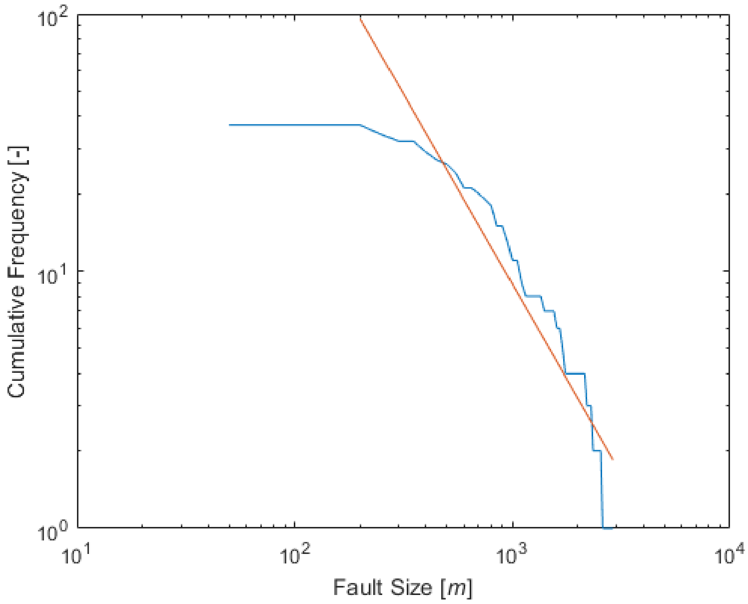

Figure 53. Fracture length vs cumulative frequncy plot of the North Sea Group horizon in log- log scale.

7

Discussion

7.1 First Steering Cube

This chapter focuses on describing, interpreting and comparing the results of the data faults and fractures form targeted horizons of the first Steering Cube, the comparison is made between the Scruff formation and the Rijnland horizon. The second comparison is between the Chalk horizon and the North Sea Group horizon characteristics in order to understand if there are changes or similarities between the faults and fractures length scale characteristic.

7.2 Discussion Scruff horizon

As it has been explained, based on the analysis of the histograms figure 20 and the rose diagram (figure 21), is evident that faults and fractures that that belong to the range of 0 to 300 meters show a spread orientation and a high frequency at the 135º and 150º which correspond to an orientation of NNW-SSE. This trend is also seen in the range of 300 to 600 meters, this group also shows lower spread in the orientation. Finally, the faults and fractures in the range of 600 m to 900 meters also shows this orientation although not many structures characterized fall into this length group. By analyzing the rose diagram one set is defined and stablished for the Scruff horizon, the set characteristics shown in table 4 demonstrate that this set contain structures belonging to the 3 different length groups belonging to the orientation range of 135º and 150º.

In order to analyze the fault network style, the Scruff horizon is analyzed in the smallest scale present due to this problem a interpolation is required in order to generate the surface, the interpolation linked both patches and allowed to see a straight line crossing the salt wall. In this interpolated horizon the style of polygonal faulting can be seen. The horizon is interpolated hence appears as a flat line allowing to visualize the characteristics if the fault and fracture network as if it was a z slice. Regarding the power of law value is -2.25.

Regarding the geometry of the fault and fractures they follow the trend of the big scale features described in chapter. As the trend in NNW-SSE. In the part where the faults and fractures were interpreted. At the Scruff horizon level and crossing the salt structure a polygonal faulting can be seen. This in comparison with the horizons above the Scruff formation similar as they also follow this orientation.

7.3 Discussion of the Rijnland horizon

With the analysis of the length distribution histograms and the rose diagram plot, two sets of faults and fractures have been established for the Rijnland horizon (table 7). The first length group between 0 to 300 meters show a spread distribution for individual structures, as well with high frequency peaks in the range showing an orientation NNW-SSE between the orientation of 120º and 145º. For the length range of 300 m to 600 m a lower frequency of faults and fractures with the orientation of 165º to 185º is encountered. For the range belonging to 600 m to 900 m the trend is kept for the orientation 120º and 140º and only a couple structures for the orientation of 165º and 185º which is mostly pointing North-South direction, this set is mostly found in the western part of the study area and far from the salt structure. For the Rijnland horizon the set with orientation of 120º and 145º are mostly structures that follow a trend with respect to the length axis of the salt structure (figure 4) that is present in the area. this means that that there may be a relation with the deeper faults as thick-skinned systems faults usually show a lateral offset, which is mostly in the footwall. Finally, for the style that is seen of the fracture network it is clear that a pattern of polygonal faulting can be seen in the area where the salt wall is present, this is the same with the Scruff formation where the interpolation of the horizon creates a flattened horizon that does not necessary follows a "topography" but allows to visualize the information as if it was a z slice. The value regarding the slope the power of the Rijnland formation is -2.838 a much steeper trend line is seen, and the fitting line validates the length distribution for lengths from 200 meters until 1000 meters. This difference is explained due to the fact that more sampling is done in the Rijnland as the area where is present is bigger hence the sampling influences as the cumulative frequency curve is smother than the Scruff.

7.4 Comparison of Scruff horizon and Rijnland horizon

The main difference that is encountered is the number of faults and fractures present in each horizon where the Rijnland formation accounts for a higher frequency of structures. This can be seen comparing the cumulative frequency distribution as the Rijnland cumulative curve is smoother as the frequency of structures increases due to more sampling, As well the lengths that the powers of law validate are lower with the Scruff formation, This may be due to the fact that the Scruff formation contains a much higher amount of structures between 0 and 300 meters, while the Rijnland horizon accounts for high frequencies in the lowest length range but as well high frequency in the medium scale. Regarding the style of faulting present in this horizon both share the characteristically polygonal faulting encountered in the area. Regarding the orientation the Scruff formation has one set that is oriented between 135º and 150º this orientation range is broadened in the Rijnland horizon from 120º and 145º.

7.5 Discussion of Chalk horizon

Two sets have been defined for the Chalk horizon based on the analysis of the histograms and the rose diagram plot. The set with orientation of 120º and 145º tend to be present in all length ranges analyzed. This trend is mostly for medium scale and large-scale features as they tend to follow a parallel trend with the longest axis of the salt structure.

The large-scale faults that follow the thick skinned soft linked faults described in chapter 2 also follows the trend of 120º and 145º. For the smallest scale features is evident that a polygonal style of faulting exists above of the salt structure. The concentration is much less than the amount encountered in Rijnland or Scruff formation. This explains the spread orientations in the lowest length range as this feature enter in this scale. This style of faulting is also present in the interpolated area of the Scruff and Rijnland formation that are deeper. For the range between 900 and 1200 meters fractures enter to the trend observed in previous length groups of 120º and 145º.

Finally, the larger scale structures above 1200 meters enter into this same orientation of 120º to 145º.This is similar as Rijnland horizon that tend to follow this orientation, although in comparison with the Rijnland horizon the orientation North-South set also appears in the Chalk horizon with a higher frequency. This set mostly describe the faults and fractures at the West of the salt wall. In the end of the salt structure, a characteristic radial pattern appears, hence showing that there are lateral changes with respect the orientation as we move far from the salt structure. The set belonging to the range between 120º and 145º in the Chalk group are faults near the salt crest and follow the length axis of the sault structure as well. Regarding the power of law, the exponent value of the slope is -2.3and the trend line describes the length distribution in the length range of 200 meters to 1600 meters.

7.6 Discussion of the North Sea Group horizon

Three sets of faults and fractures have been found based on the analyses of the length distribution histograms and the rose diagram plot. From the different sets that are encountered the one with highest frequency belong to the orientation range of 120º and 150º. Which is an orientation trend followed as well in the other horizons. This is due to the fact that the faults in medium scale and large scale follows a parallel orientation of the length axis of the salt wall. The set number two in table 13 mostly oriented to North-South in this set different length ranges are included. The faults that follow this trend are mostly located in the edge of the salt structure south from the Steering cube I and in the west part of the study area large scale fault follows exactly this trend. Again, the radial pattern of faults can be seen in the tip of the salt wall as in the Chalk group horizon. A polygonal style of faulting can be recognized in the horizon which is linked to the small scale sparse orientation although is less than all the previous horizons. Regarding the Power of law exponent which is -2.34 the fitting curve shows a high slope that fits to the cumulative distribution in the lowest range possible which is 200 m to 1000 meters.

7.7 Second Steering Cube

For the second part of this chapter the discussion of the second steering cube is made. In this seismic volume only the Rijnland, Chalk and North Sea Group horizons are present. In this chapter the comparison of the length scale characteristics, length distribution and sets are compared between the three horizons.

7.8 Discussion of Rijnland Horizon

For the Rijnland horizon two sets of faults have been encountered. The first set follows a trend ranging from 75º and 95º orientation, the second range is between 105º and 120º. In the first set different lengths ranges are found this can be validated by analyzing the orientation histograms in 39. For the small-scale features of this horizon that are outside this set, a spread orientation can be distinguished as well as low frequency. Analyzing the set number 1, contains the highest frequency with 30 structures and a mean length of 858.26 m in comparison with the set number two where the mean length is 641.90 meters and lower frequency. The length range with highest frequency is 600 to 900 meters with 23 structures encountered and peak frequencies at 75º to 95º. For set number two as length tends to increase the frequency decreases. The trend can be defined for the first set as East-West orientation. Except for a couple of structures that are located at the North of the area of interest which follow a NNW-SSE orientation. The style of the large-scale faults is defined as defined as conjugate fault pattern, for validation see vertical section in Chapter 5 figure 10. For the fault and fracture network next to the damage zone of the large-scale features can be described as anastomosing faults. Regarding the Power of law exponent which is -2.905 the fitting curve shows a high slope that fits to the cumulative distribution in the range from 300 to 1000 meters. It is clear that the faults are following the crest of the salt structure

7.9 Discussion of Chalk Group horizon

For this horizon only one set of faults and fractures is defined, the set orientation is in the range of 75º and 95 º which can be seen in the rose diagram and compared with the orientation of the faults and fractures at the different length ranges from the histogram in figure 45. The number of fractures characterized is 33 and the mean length is 541.26 meters. With set of structures maintaining an East-West Orientation this matches with the main length axis of the salt structure described in the sketch of the vertical section in figure 4.Large scale faults follow a conjugate geometry this mayor faults affect the Rijnland horizon beneath the Chalk and the North sea above. As we analyze the medium scale features a characteristic anastomosing style of fracture appears, is a characteristic that is shared with the Rijnland horizon. Finally, the Power of law exponent is -3.26 the fitting curve shows a high slope that fits to the cumulative distribution in the range from 250 to 1200 meters.

7.10 Discussion of the North Sea horizon

For this horizon only one set of faults and fractures is defined, the set orientation is in the range of 78.5º and 105 º which can be confirmed in the rose diagram figure 52 and compared with the orientation of the faults and fractures at the different length ranges from the histogram in figure 51. The number of fractures characterized is 31 and the mean length is 996.26 meters. This set keeps maintaining an East-West Orientation this matches with the main length axis of the sketch salt structure described in vertical section figure 4 and are located in the crest of the salt wall. Large scale faults follow a conjugate geometry, this mayor faults affect the North Sea Group horizon and the horizons beneath it. A similarity encountered with the other horizons is the anastomosing style (Peacock D.C.P, Nixon C.W, Rotevatn A., Sanderson D.J., & Zuluaga, 2016) of fracture that follow the main conjugate faults near the damaged area. Finally, the Power of law exponent is -2.55 the fitting curve shows a high slope that fits to the cumulative distribution in the range from 350 to 1200 meters.

8

Conclusion

The application of geometrical attributes has delivered an enhanced framework for the accurate fault and fracture interpretation over specific horizons belonging to the Jurassic and the Cretaceous, located in the F10 block offshore the Netherlands. The attributes that delivered the most optimal and realistic representation of faults and fractures were the Similarity evaluated with the Fault Enhancement Filter, the different curvatures like Most Positive Curvature, Maximum Curvature, Most Negative Curvature and the newly developed Thinned fault likelihood. Using the software OpendTect created by dGB Earth Sciences and following the methodology proposed by (Jaglan Hardeep, 2016) an improved the interpretation of this structural features in the seismic survey was done introducing the structural dip data to the generation of the geometrical attributes. The creation of seismic volume determined as Steering Cube that contained and honored the information of the structural dip, is a volume that improved the delineations and visualization of faults by removing the noise from the seismic reflectors. Two Steering cube were developed the Background steering cube which is a heavily smoothed volume that honors the overall trend determined as structural dip and the Detailed Steering cube that is moderately filtered proved to define local dip trends. The application of the Structural oriented filters Dip Steered Median Filter that enhances the seismic amplitude and the Dip Steered Diffusion Filter that enhances the diffusion in the proximity of the fault were applied to generate a consequent filter determined as Fault Enhancement Filter. This filter was used to generate a new similarity attribute that demonstrated better fault and fracture delineation and better visualization than without application of the Steering cube and filters generating more confidence when interpreting the faults and fractures. The generation of curvature attributes using the Detailed Steering Cube allowed to visualize structural features like the upthrown or downthrown side of the fault, this curvature attributes works as reference for determining faults and fractures that would not be visible with other attributes. The creation of the Thinned Fault Likelihood that is an automated fault extraction method based on the semblance of the seismic data, proved to be a great contribution for the analysis of the faults and fractures. This attribute created a new measurement based on the evaluation of the semblance scanned along the dips and strikes allowing to use it as a confirmation of the faults and fractures in the seismic data. Further unconventional attributes were calculated with this thinned fault likelihood filter as an input, this unconventional attribute are fault density and fault proximity.

8.1 Recommendations

The use of OpendTect and the methodology proposed by (Jaglan Hardeep, 2016) can deliver sharper, and better delineated faults and fractures if used with the dip and azimuth of the seismic volume. The evaluation of the different steering cubes should be done based on the characteristics of the seismic survey due to the fact that each survey is acquired with its own bin size configuration. When the Steering cubes are created the software OpendTect with the algorithm applies filters and uses mean statistics with the in lines ad crosslines indicated by the user. The user should test the best option instead of following only a rule of thumb value for the spacing of the In lines, Cross lines and z in milliseconds. Finally, a methodology to generate a velocity models and to migrate to depth would provide more information of the position of the faults and fractures, impacting the fault and fracture characterization. The creation of the Thinned Fault Likelihood attribute can generate great insight of the information contained inside the seismic survey, most import this new method of fault and fracture automated extraction can be used as discrimination method for faults and fractures with throws under the seismic resolution. Attention should be kept for the sensibility of this attribute as unrealistic faults can be created. In order to create a better more realistic Thinned Fault likelihood result is necessary to constrain the thinned likelihood with the correct geological dip and azimuth of the signal, this because thinned fault likelihood attribute is very expensive to create term of machine computing. The application of cut off values with OpendTect has to be tested as in some cases faults and fractures can be smoothed to much hence erasing faults that normally would be there.

9 Appendix

9.1 Steering Cube I

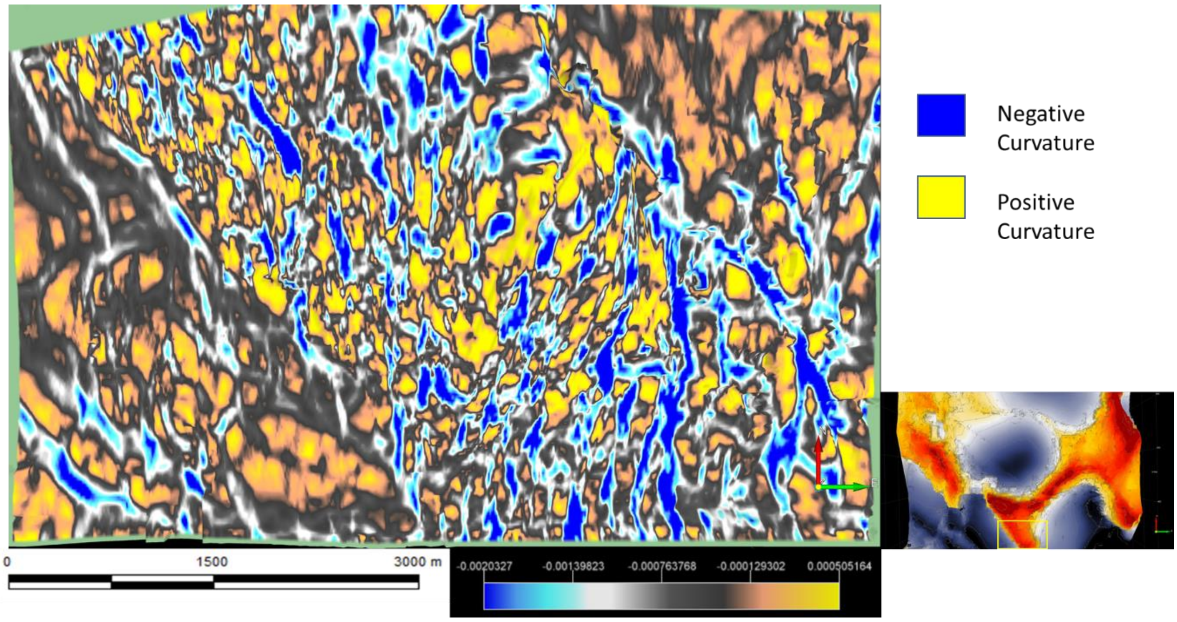

Figure 54.Most negative curvature Scruff horizon.

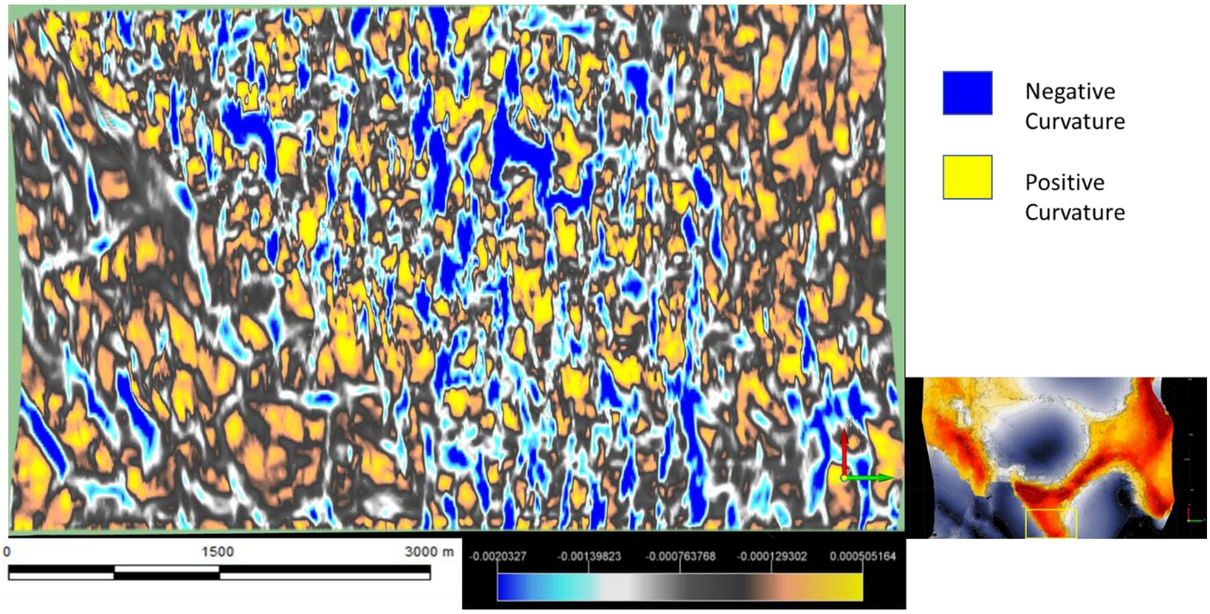

Figure 55.Most negative curvature Rijnland horizon.

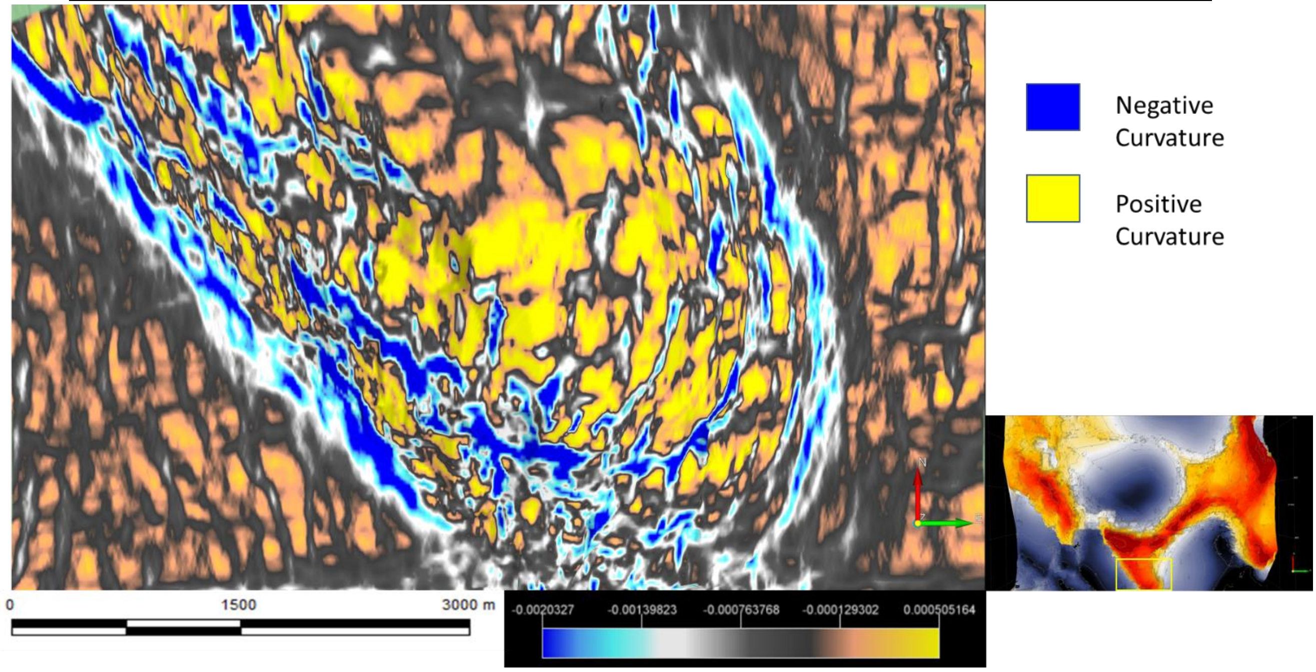

Figure 56.Most Negative Curvature Chalk horizon.

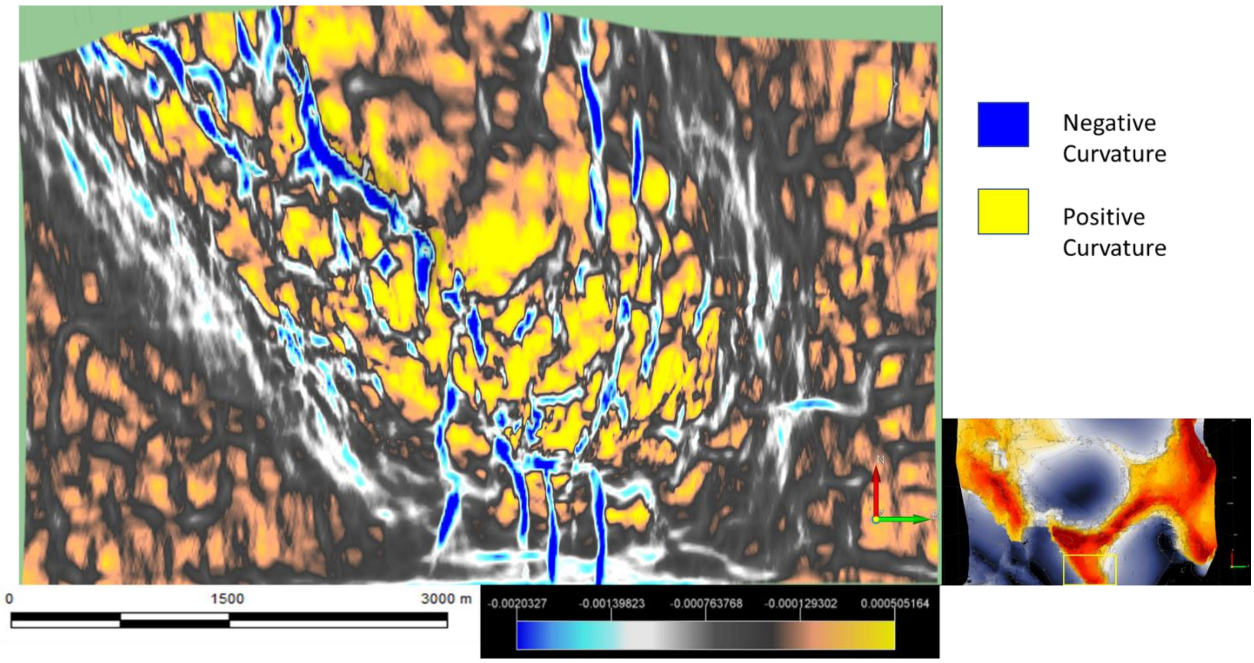

Figure 57. Most Negative Curvature North Sea Group horizon.

9.2 Second Steering Cube II

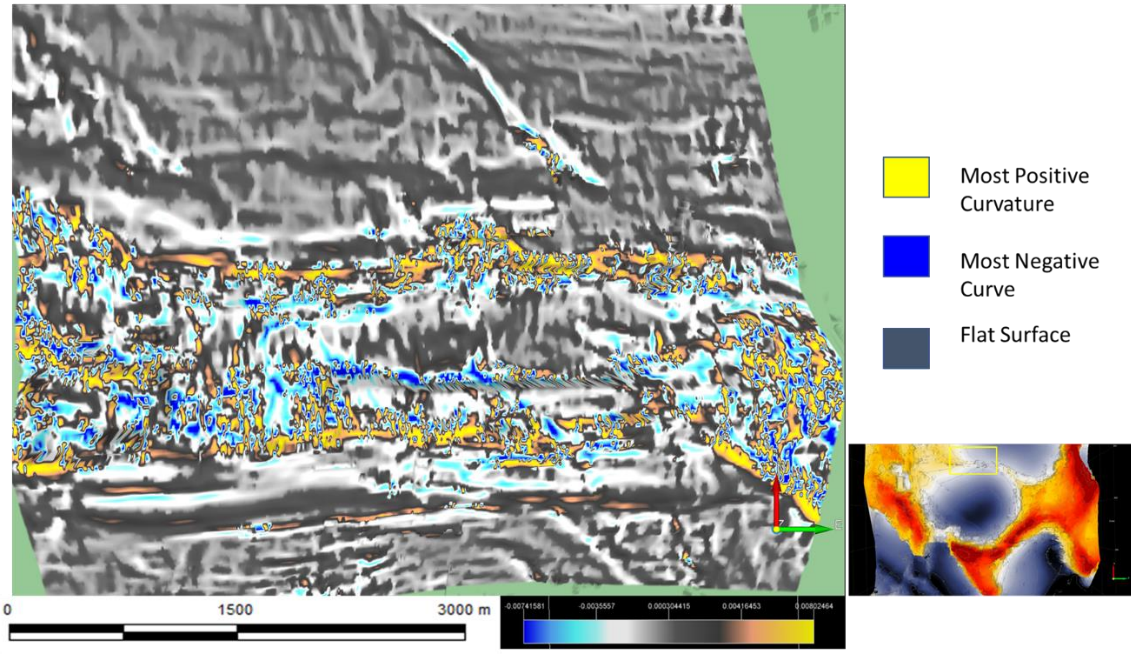

Figure 58.Most Negative Curvature Rijnland horizon.

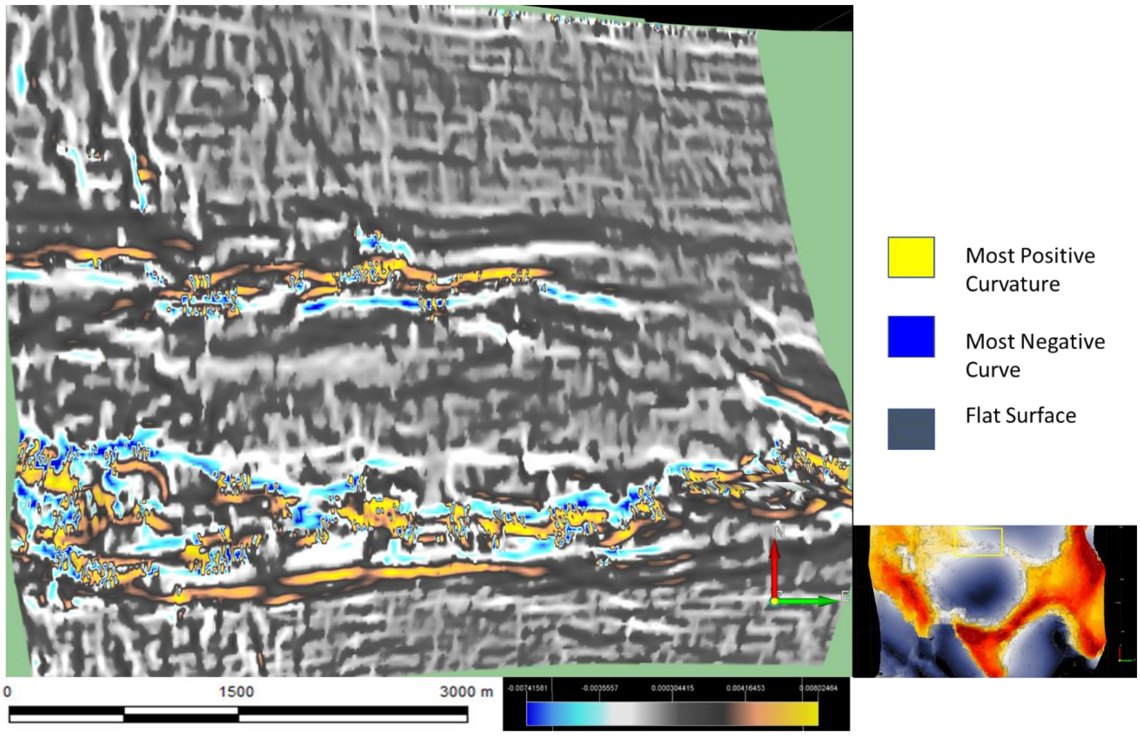

Figure 59.Most Negative Curvature Chalk Group.

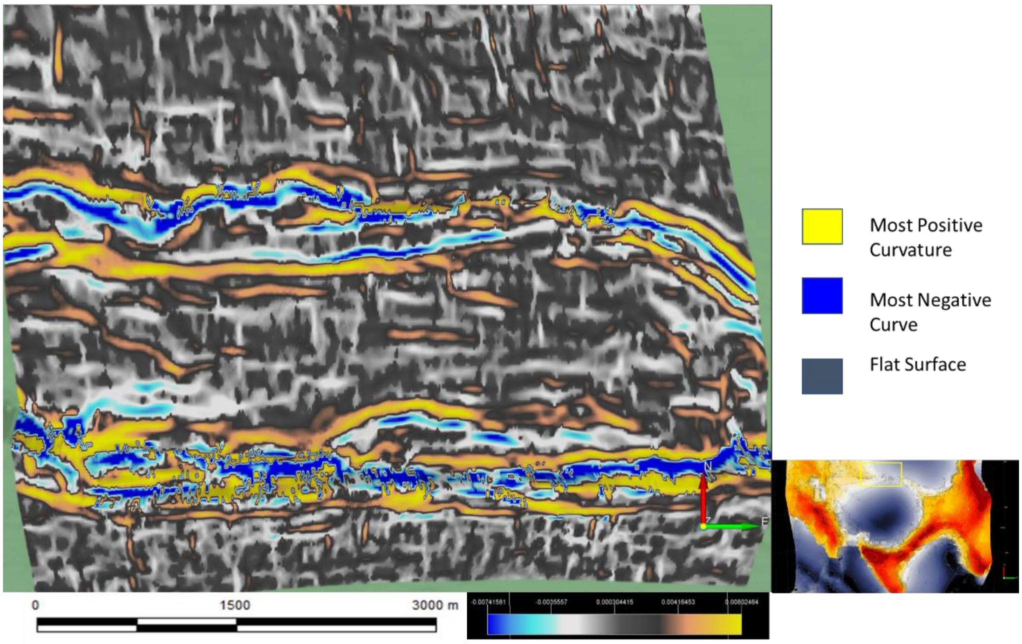

Figure 60.Most negative Curvature North Sea Group

BIBLIOGRAPHY

Bonnet, E., Bour.O, Odling, E. N., Davy, P., Main, I., Cowie, P., & Berkowitz, B. (2001). Scaling of Fracture Systems in Geological Media. *Reviews of Geophysics 39*, 347-383.

Hale, D. (2013). Methods to compute fault images, extract fault surfaces, and estimate fault throws from 3D seismic images. (pp. 33-43). First Break.

I. D. Bartholomew, J. M. (1993). Regional structural evolution of the North Sea: oblique slip and the reactivation of basement lineaments. *Petroleum Geology Conference series* (pp. 1109-1122). London: Geological Society.

J. de Jager, T. W. (2007). Geology of the Netherlands. Herent, Belgium: Royal Netherlands Academy of Arts and Sciences.

J.H. ten Veen, S. v. (2012). Thin- and thick-skinned salt tectonics in the Netherlands; a quantitative approach. *Netherlands Journal of Geosciences*, 447-464.

Jager, J. d. (2003). Inverted basins in the Netherlands, similarities and differences. *Netherlands Journal of Geosciences*, 355-366.

Jaglan Hardeep, R. H. (2016). Fault and Fracture Detection in Unconventional Reservoirs: A Utica Shale Study. *Unconventional Resources Technology* (pp. 03-09). San Antonio, Texas: SPE, AAPG, SEG.

M.C. Geluk, M. W. (2007). Geology of the Netherlands. Herent, Belgium: n.v. Peeters s.a.

Marfurt, C. S. (2007). Preconditioning seismic data with 5D interpolation for computing geometric attributes. *The Leading Edge*, 1456–1460.

Oliver B. Duffy, R. L. (2013). Mobile evaporite controls on the structural style and evolution of rift basins:Danish Central Graben,North Sea. *EAGE*, 310-330.

Opperman, R. (2012). New Method for Seismic Identification of fluid Conduits or Barriers Challenges Seeral Industry Paradigms. *AAPG/SPE/SEG Hedgeberg Research Conference* (pp. 1-5). Provence, France: OPPtimal Exploration & Development Pty Ltd.

Oppermann, R. (2012). Finding Sweet Spots through Seismic Fracture Extraction - Unconventional Case Studies from Around the World. *SPE Asia Pacific Oil and Gas Conference and Exhibition* (pp. 1-8). Perth, Australia: Society of Petroleum Engineers International.

Paul de Groot, T. (2003). Post-stack dip- and azimuth processing. *Journal of Seismic Exploration*, 113-126.

Peacock D.C.P, Nixon C.W, Rotevatn A., Sanderson D.J., & Zuluaga, L. (2016). Glossary of fault and other fracture networks. *Journal of Structural Geology*, 12-29.

Petukhov A.V., E. S. (2015). New Technologies of development of Austin Chalk and Buda Low-Porous. *VNIGRI International Conference on Unconventional Hydrocarbons* (pp. 1-9). St.Petersburg: Russia Petroleum Research Exploration Institute.

Qayyum F, J. H. (2015). Unconventional seismic attributes for fracture characterization. (pp. 101-109). First Break.

Roberts, A. (2001). *Curvature Attributes and their application to 3D Interpreted Horizons.* Stavanger, Norway: Enterprise Oil Norge Ltd.

Roberts, A. (2001). Curvature attributes and their application to 3D interpreted horizons. (pp. 85-100). First Break.

Seon, Y. D. (2004). The relationship between displacement and length of faults: a review. *Earth Science Review*, 317-334.

Stewart, S. (2007). Salt tectonics in the North Sea Basin: a structural style template for seismic interpreters. London: Geological Society Special Publication.

Tingdahl Kristofer M., M. d. (2005). Semi-automatic detection of faults in 3D seismic data. *Geophysical Prospecting,*, 533–542.

Verduzco, F. S. (2010). Unsteady and Pseudo-steady State Characterizationof Matrix and Fracture System for Multiple Size Blocks with the use of empirical Correlations. *Society of Petroleum Engineering International*, 1-5.

Winden, M. v. (2015). Salt Tectonics in the Northern Dutch Offshore. Utrecht: MSc. Thesis.

Wride, V. (1995). Structural features and structural styles from the Five Countries Area of the North Sea Central Graben! *EAGE*, 395-407.

Zanella E., C. M. (2003). Petroleum Geology of the Central and Northern North Sea. Geological Society of London.

Ziegler, P. A. (1990). *Geological Atlas of Western and Central Europe.* Shell Internationale Petroleum Maatschappij B.V.